Lecture 6

Rock Failure in compression, tension and shear
(13, 20 April 2020)

Ki-Bok Min, PhD

Professor
Department of Energy Resources Engineering
Seoul National University

SEOUL NATIONAL UNIVERSITY

Introduction
Outline

- Importance
  - Understanding rock failure is the foundation for the reservoir geomechanics
  - Compression
  - Tension
  - Shear
- Different loading conditions
  - Hydrostatic
  - Uniaxial
  - Triaxial
  - Polyaxial (true triaxial)

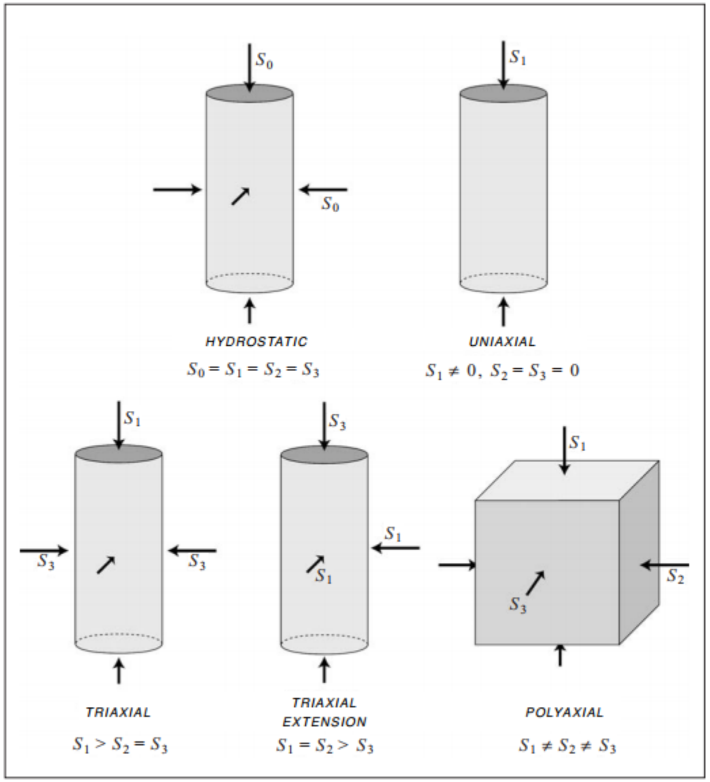

Figure 4.1. The most common types of rock mechanics tests. While it is common for petrophysical properties to be measured as a function of hydrostatic pressure, strength is typically measured via either uniaxial or triaxial tests. As discussed in the text, triaxial extension and polyaxial tests are rare. Pore pressure is frequently accommodated as an independent variable in these tests by using a flexible, impermeable sleeve outside the sample. For obvious reasons, pore pressure is not used in uniaxial tests. It is also not used in polyaxial tests because of the experimental difficulty of sealing pressure within the samples.

Zoback MD, 2007, Reservoir Geomechanics, Cambridge University Press

Introduction
Loading condition in (reservoir) geomechanics

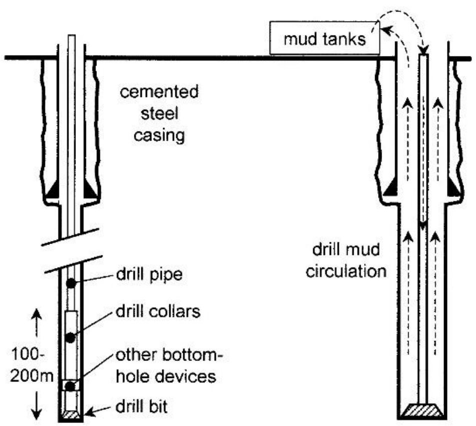

Nature of Underground Geomechanics

Civil structural problems:
Mechanics of “Addition”, “Uniaxial”

Underground Geomechanics problems:
Mechanics of “Removal”, “polyaxial”

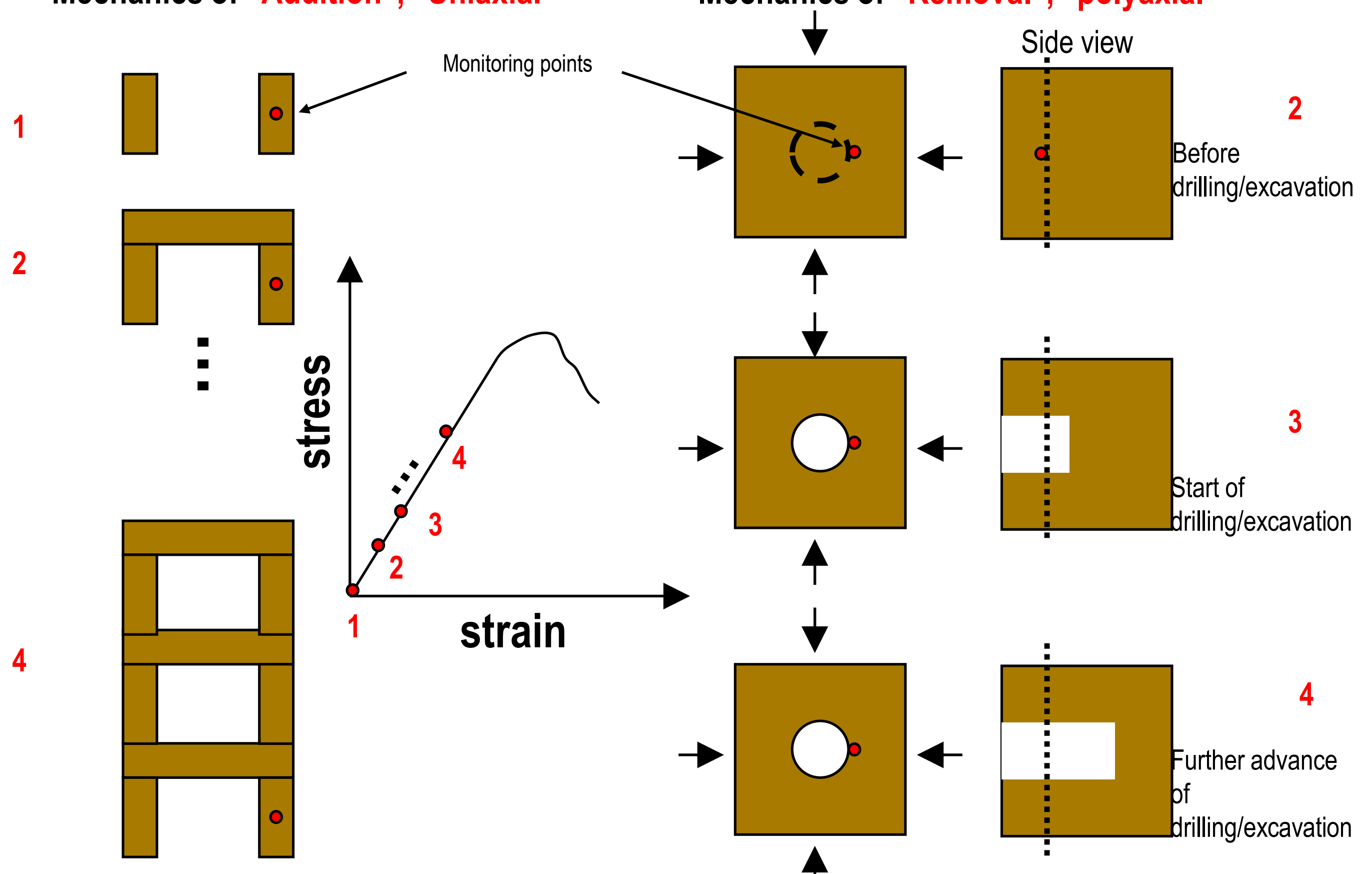

Rock strength in compression
Friction on rock surface - Friction coefficient

SEOUL NATIONAL UNIVERSITY

- Friction
  - Phenomenon by which a tangential shearing force is required in order to displace two contacting surfaces along a direction parallel to their nominal contact plane
  - Importance: friction between grains, fracture and fault

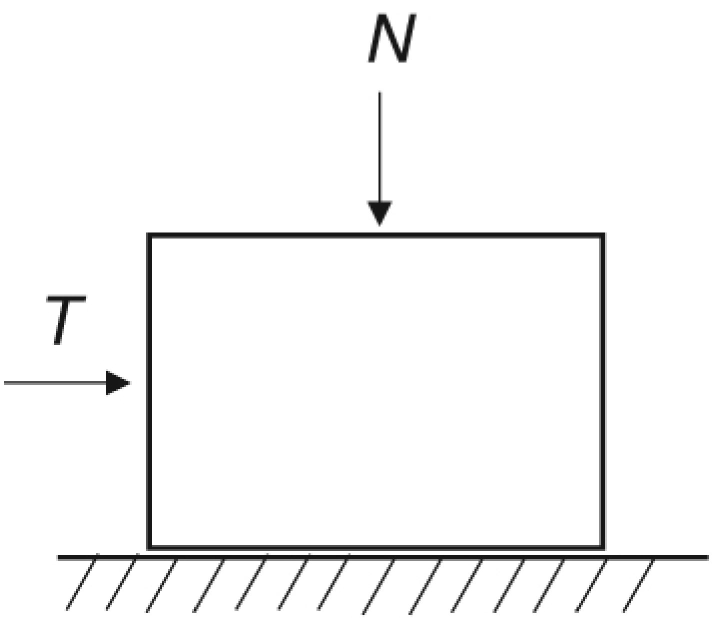

$\tau = \mu\sigma$

τ : shear stress

σ : normal stress

μ : coefficient of friction

Also called 'friction angle'. Why?

$\tau = \mu_d\sigma$

μ_d : coefficient of dynamic friction

Jaeger, Cook and Zimmerman, 2007, Fundamentals of Rock Mechanics, 4th ed., Blackwell Publishing

Rock strength in compression
Friction on rock surfaces - Friction coefficient

SEOUL NATIONAL UNIVERSITY

- Friction angle

$$\mu = \tan\phi$$

$$\phi = \text{friction angle}$$

DETERMINING μ_s EXPERIMENTALLY

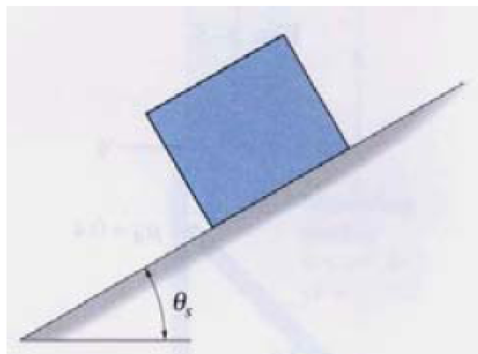

A block with weight **W** is placed on an inclined plane. The plane is slowly tilted until the block just begins to slip.

The inclination, θ_s, is noted. Analysis of the block just before it begins to move gives (using $F_s = \mu_s N$):

FBD:

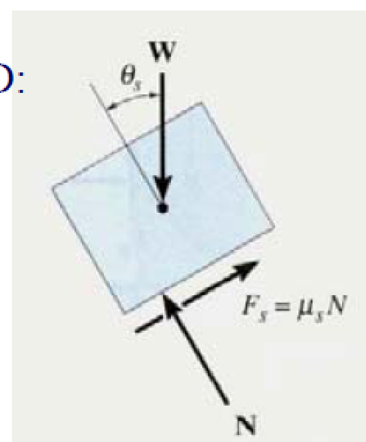

$$\nwarrow + \quad \sum F_y = N - W\cos\theta_s = 0$$

$$\nearrow + \quad \sum F_x = \mu_s N - W\sin\theta_s = 0$$

Using these two equations, we get μ_s = $(\mathbf{W}\sin\theta_s)/(\mathbf{W}\cos\theta_s) = \tan\theta_s$
This simple experiment allows us to find the μ_s between two materials in contact.

Rock strength in compression
Friction on rock surface - cohesion

- Coulomb failure criterion (on fractures)

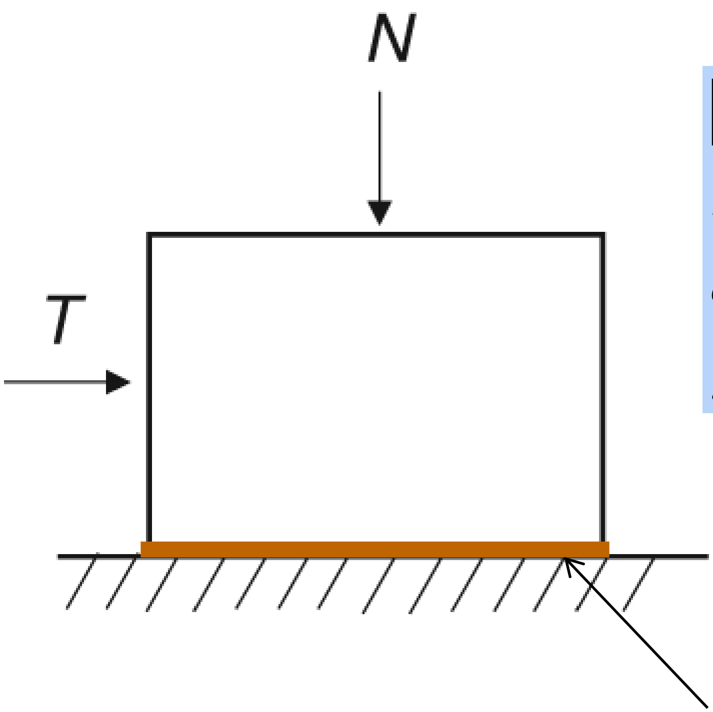

$$|\tau| = S_0 + \mu\sigma = S_0 + \sigma\tan\phi$$

S_0 : cohesion (often, c is used), or 'shear strength'

ϕ: friction angle

μ : coefficient of friction angle

Glue or something

Jaeger, Cook and Zimmerman, 2007, Fundamentals of Rock Mechanics, 4th ed., Blackwell Publishing

Rock strength in compression

SEOUL NATIONAL UNIVERSITY

- The failure of rock in compression
  - Complex process: creation of small tensile crack and frictional sliding on grain boundaries
  - We assume that are infinite number of fictitious fracture within intact rock

$$\tau_f = 0.5(\sigma_1 - \sigma_3)\sin 2\beta \qquad (4.1)$$

$$\sigma_n = 0.5(\sigma_1 + \sigma_3) + 0.5(\sigma_1 - \sigma_3)\cos 2\beta \qquad (4.2)$$

where β is the angle between the fault normal and σ_1 (Figure 4.2a).

$$\tau = S_0 + \sigma_n \mu_i \qquad (4.3)$$

As cohesion is not a physically measurable parameter, it is more common to express rock strength in terms of C_0. The relationship between S_0 and C_0 is:

$$C_0 = 2S_0\left[\left(\mu_i^2 + 1\right)^{1/2} + \mu_i\right] \qquad (4.4)$$

  - μ_i: coefficient of internal friction
  - UCS, C_0: unconfined uniaxial compressive strength

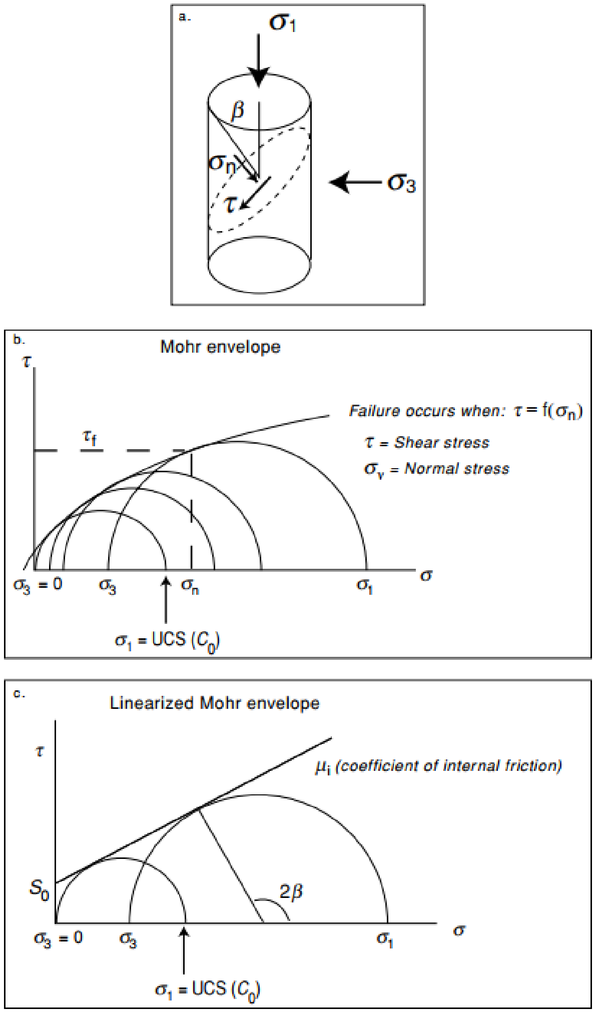

Figure 4.2. (a) In triaxial strength tests, at a finite effective confining pressure σ_3 (S_3–P_0), samples typically fail in compression when a through-going fault develops. The angle at which the fault develops is described by β, the angle between the fault normal and the maximum compressive stress, σ_1. (b) A series of triaxial strength tests at different effective confining pressures defines the Mohr failure envelope which typically flattens as confining pressure increases. (c) The linear simplification of the Mohr failure envelope is usually referred to as Mohr–Coulomb failure.

Zoback MD, 2007, Reservoir Geomechanics, Cambridge University Press

Rock strength in compression

SEOUL NATIONAL UNIVERSITY

- Linearized Mohr failure envelope

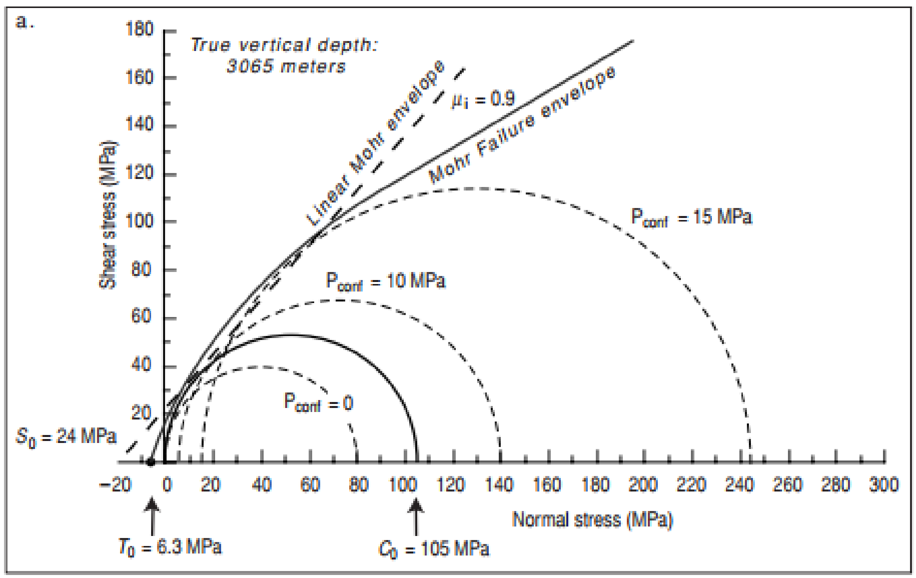

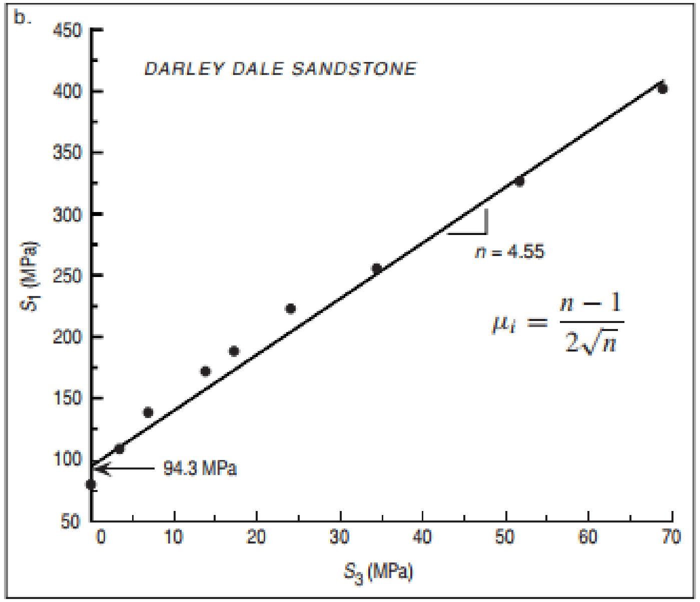

Zoback MD, 2007, Reservoir Geomechanics, Cambridge University Press

Rock strength in compression

SEOUL NATIONAL UNIVERSITY

- Cohesion (S_o)
- Coefficient of Internal friction (μ_i)

$$\sigma_1 = C_0 + q\sigma_3 \tag{4.6}$$

where C_0 is solved-for as a fitting parameter,

$$q = \left[\left(\mu_i^2 + 1\right)^{1/2} + \mu_i\right]^2 = \tan^2(\pi/4 + \phi/2) \tag{4.7}$$

and

$$\phi = \tan^{-1}(\mu_i) \tag{4.8}$$

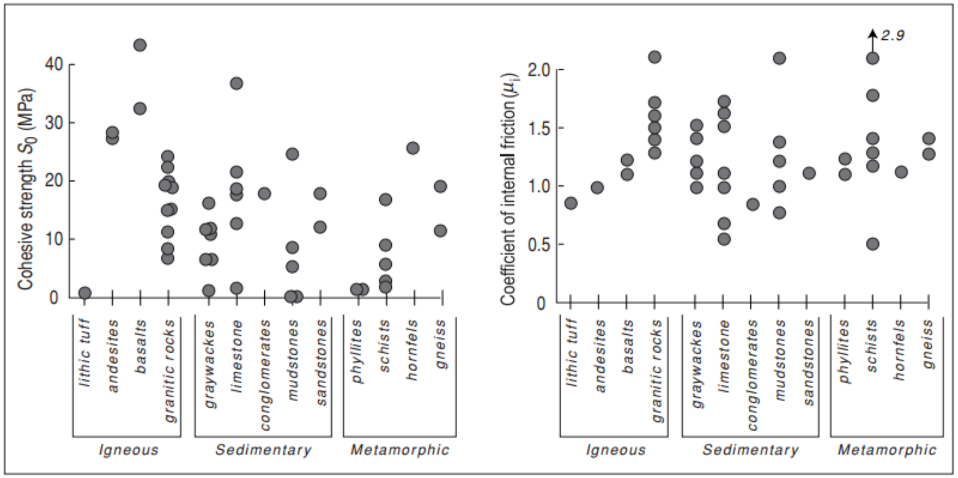

Figure 4.4. Cohesion and internal friction data for a variety of rocks (data replotted from the compilation of Carmichael 1982). Note that weak rocks with low cohesive strength still have a significant coefficient of internal friction.

Zoback MD, 2007, Reservoir Geomechanics, Cambridge University Press

Rock strength in compression
Importance for borehole stability

SEOUL NATIONAL UNIVERSITY

- Application of failure criterion to borehole stability
  - Role of mud weight increase

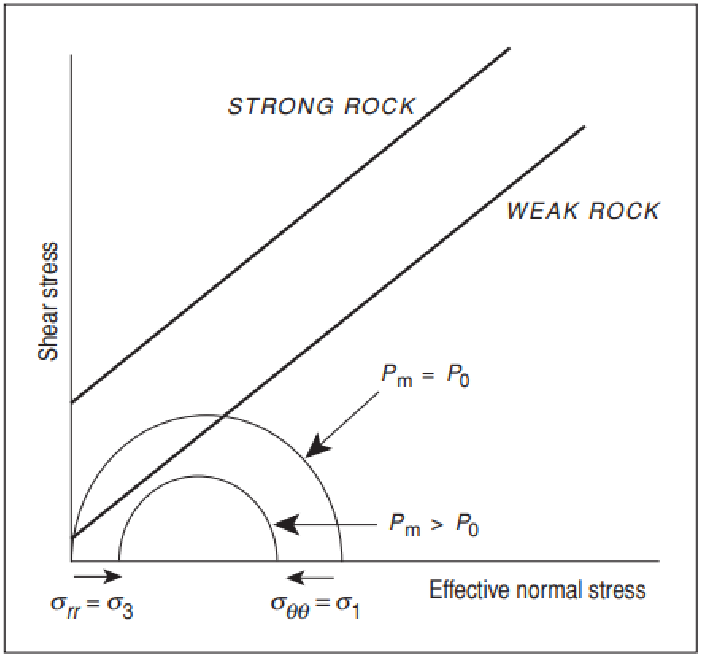

Figure 4.5. Schematic illustration of how raising mud weight helps stabilize a wellbore. The Mohr circle is drawn for a point around the wellbore. For weak rocks (low cohesion), when mud weight and pore pressure are equal, the wellbore wall fails in compression as the radial stress, σ_{rr} is equal to 0. Raising mud weight increases σ_{rr} and decreases $\sigma_{\theta\theta}$, the *hoop stress* acting around the wellbore. This stabilizes the wellbore by reducing the size of the Mohr circle all around the circumference of the well.

Zoback MD, 2007, Reservoir Geomechanics, Cambridge University Press

Rock strength in compression
Various criteria

SEOUL NATIONAL UNIVERSITY

- Various failure criteria exist
  - Linearized Mohr-Coulomb $\sigma_1 = C_0 + q\sigma_3$
  - Hoek-brown criterion $\sigma_1 = \sigma_3 + C_0\sqrt{m\frac{\sigma_3}{C_0} + s}$
  - Modified Lade criterion
  - Modified Wiebols-Cook criterion
  - Drucker-Pager criterion
- Linear vs. non-linear
- Consideration of the intermediate principal stress

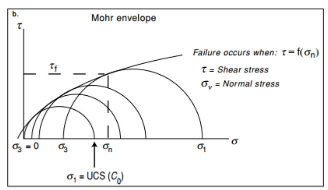

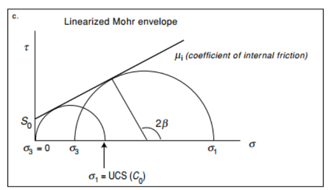

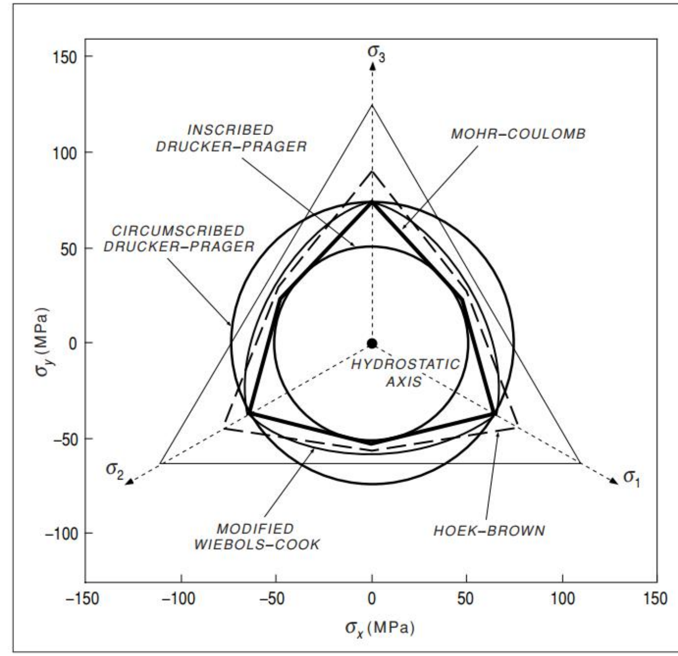

Figure 4.6. Yield envelopes projected in the π-plane for the Mohr–Coulomb criterion, the Hoek–Brown criterion, the modified Wiebols–Cook criterion and the circumscribed and inscribed Drucker–Prager criteria. After Colmenares and Zoback (2002). *Reprinted with permission of Elsevier.*

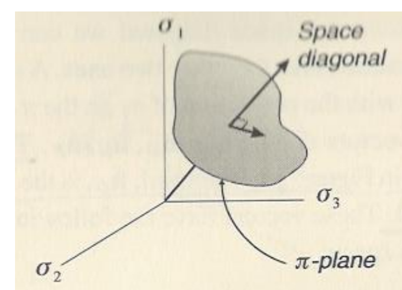

π-plane: plane perpendicular to the straight line $\sigma_1=\sigma_2=\sigma_3$

Zoback MD, 2007, Reservoir Geomechanics, Cambridge University Press

Linearized Mohr Coulomb Failure criterion

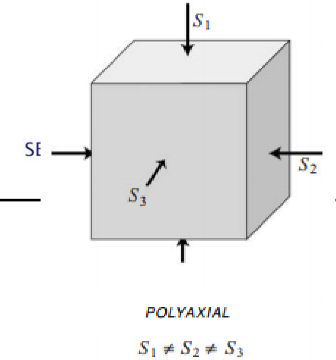

- Best fitting failure criteria (Colmenares and Zoback, 2002)
  - Dunham dolomite (백운석)
  - solenhofen limestone (석회암)
  - Shirahama sandstone (사암)
  - Yuubari shale (셰일)
  - KTB amphibolite (각섬암)
- Linear Mohr Coulomb

$$\sigma_1 = C_0 + q\sigma_3$$

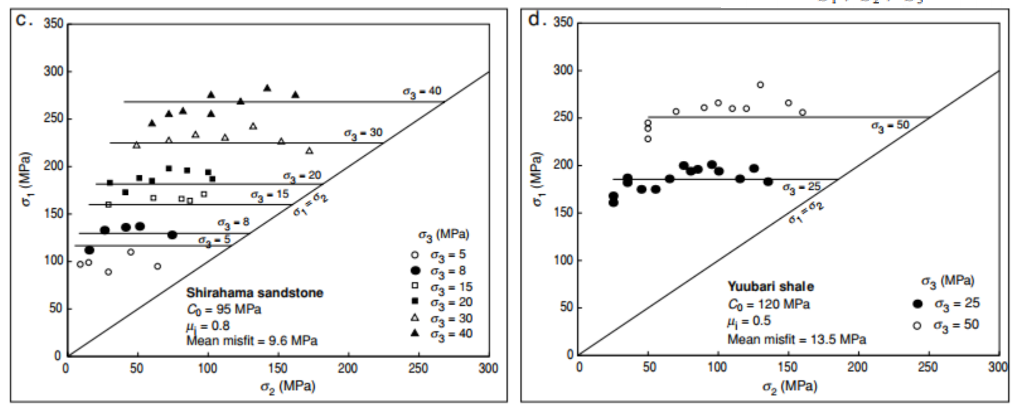

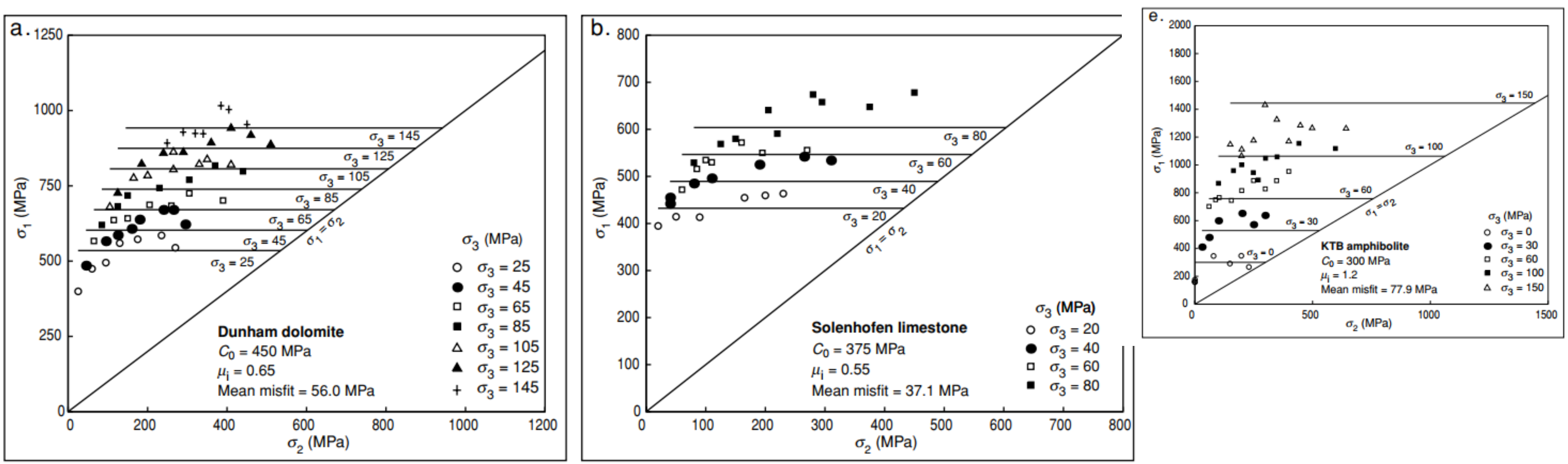

Zoback MD, 2007, Reservoir Geomechanics, Cambridge University Press

Hoek-Brown failure criterion

- Non-linear form
  - Obtaining m is not straightforward from geophysical well logs

$$\sigma_1 = \sigma_3 + C_0\sqrt{m\frac{\sigma_3}{C_0} + s} \tag{4.9}$$

where m and s are constants that depend on the properties of the rock and on the extent to which it had been broken before being tested. Note that this form of the failure law

- $5 < m < 8$: carbonate rocks with well-developed crystal cleavage (dolomite, limestone, marble).
- $4 < m < 10$: lithified argillaceous rocks (mudstone, siltstone, shale, slate).
- $15 < m < 24$: arenaceous rocks with strong crystals and poorly developed crystal cleavage (sandstone, quartzite).
- $16 < m < 19$: fine-grained polymineralic igneous crystalline rocks (andesite, dolerite, diabase, rhyolite).
- $22 < m < 33$: coarse-grained polymineralic igneous and metamorphic rocks (amphibolite, gabbro, gneiss, granite, norite, quartz-diorite).

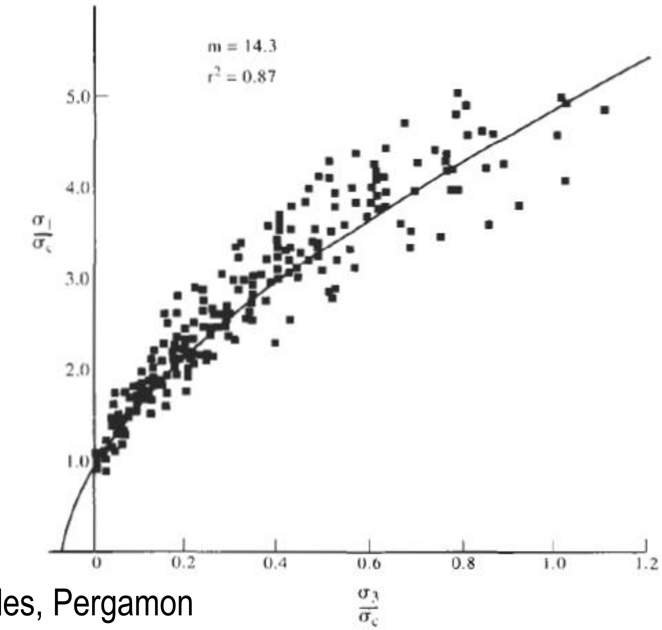

Hudson & Harrison, 1997, Engineering Rock Mechanics – An introduction to the principles, Pergamon

Modified Lade criterion

SEOUL NATIONAL UNIVERSITY

- The modified Lade criterion predicts a strengthening effect with increasing intermediate stress, followed by slight reduction

$$\frac{(I_1')^3}{I_3'} = 27 + \eta \tag{4.13}$$

where

$$I_1' = (\sigma_1 + S) + (\sigma_2 + S) + (\sigma_3 + S) \tag{4.14}$$

and

$$I_3' = (\sigma_1 + S)(\sigma_2 + S)(\sigma_3 + S) \tag{4.15}$$

S and η can be derived directly from the Mohr–Coulomb cohesion S_0 and internal friction angle ϕ by

$$S = \frac{S_0}{\tan\phi} \tag{4.16}$$

$$\eta = \frac{4(\tan\phi)^2(9 - 7\sin\phi)}{(1 - \sin\phi)} \tag{4.17}$$

where $\tan\phi = \mu_i$ and $S_0 = C_0/(2\,q^{1/2})$ with q as defined in equation (4.7).

Zoback MD, 2007, Reservoir Geomechanics, Cambridge University Press

Modified Lade criterion (Ewy, 1999)

SEOUL NATIONAL UNIVERSITY

- Modified Lade criterion
- Consideration of intermediate principal stress

$$\frac{(I_1')^3}{I_3'} = 27 + \eta \tag{4.13}$$

where

$$I_1' = (\sigma_1 + S) + (\sigma_2 + S) + (\sigma_3 + S) \tag{4.14}$$

and

$$I_3' = (\sigma_1 + S)(\sigma_2 + S)(\sigma_3 + S) \tag{4.15}$$

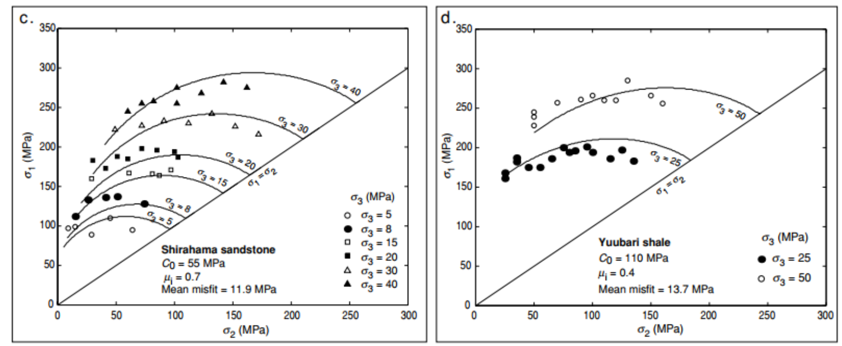

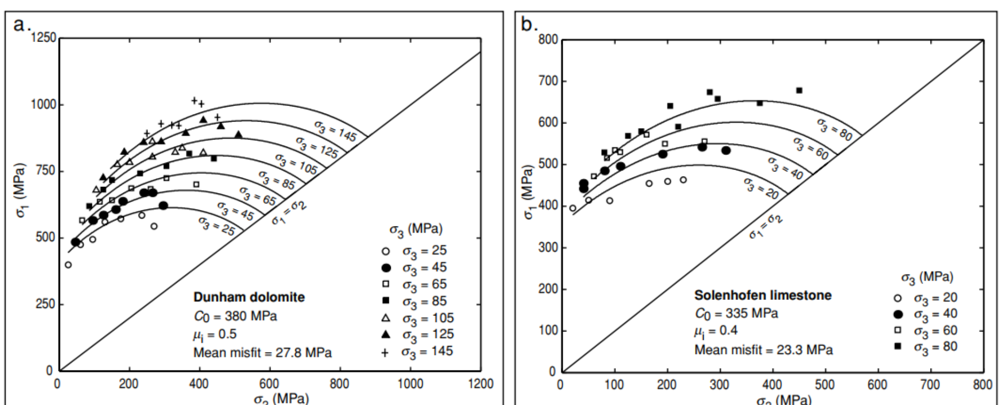

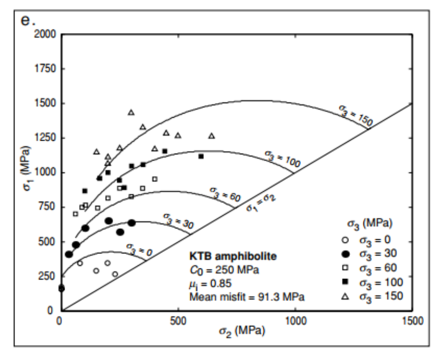

Figure 4.9. Best-fitting solution for all the rocks using the modified Lade criterion; (a) Dunham dolomite; (b) Solenhofen limestone; (c) Shirahama sandstone; (d) Yuubari shale; (e) KTB amphibolite. After Colmenares and Zoback (2002). *Reprinted with permission of Elsevier.*

Zoback MD, 2007, Reservoir Geomechanics, Cambridge University Press

Modified Wiebols-Cook criterion (Zhou, 1994)

SEOUL NATIONAL UNIVERSITY

The failure criterion proposed by Zhou predicts that a rock fails if

$$J_2^{1/2} = A + BJ_1 + CJ_1^2 \quad (4.18)$$

where

$$J_1 = \frac{1}{3}(\sigma_1 + \sigma_2 + \sigma_3) \quad (4.19)$$

and

$$J_2^{1/2} = \sqrt{\frac{1}{6}[(\sigma_1 - \sigma_2)^2 + (\sigma_1 - \sigma_3)^2 + (\sigma_2 - \sigma_3)^2]} \quad (4.20)$$

J_1 is the mean effective confining stress and, for reference, $J_2^{1/2}$ is equal to $(3/2)^{1/2}\tau_{\mathrm{oct}}$, where τ_{oct} is the octahedral shear stress

$$\tau_{\mathrm{oct}} = \frac{1}{3}\sqrt{(\sigma_1 - \sigma_2)^2 + (\sigma_2 - \sigma_3)^2 + (\sigma_2 - \sigma_1)^2} \quad (4.21)$$

The parameters A, B, and C are determined such that equation (4.18) is constrained by rock strengths under triaxial ($\sigma_2 = \sigma_3$) and triaxial extension ($\sigma_1 = \sigma_2$) conditions (Figure 4.1). Substituting the given conditions plus the uniaxial rock strength ($\sigma_1 = C_0$, $\sigma_2 = \sigma_3 = 0$) into equation (4.18), it is found that

$$C = \frac{\sqrt{27}}{2C_1 + (q-1)\sigma_3 - C_0}\left(\frac{C_1 + (q-1)\sigma_3 - C_0}{2C_1 + (2q+1)\sigma_3 - C_0} - \frac{q-1}{q+2}\right) \quad (4.22)$$

with $C_1 = (1 + 0.6\,\mu_i)C_0$ and q given by equation (4.7),

$$B = \frac{\sqrt{3}(q-1)}{q+2} - \frac{C}{3}[2C_0 + (q+2)\sigma_3] \quad (4.23)$$

and

$$A = \frac{C_0}{\sqrt{3}} - \frac{C_0}{3}B - \frac{C_0^2}{9}C \quad (4.24)$$

$$|\tau_{oct}| = \frac{1}{3}\left\{(\sigma_1 - \sigma_2)^2 + (\sigma_2 - \sigma_3)^2 + (\sigma_3 - \sigma_1)^2\right\}^{1/2} = \frac{\sqrt{2}}{3}\left\{I_1^2 + 3I_2\right\}^{1/2} = \sqrt{\frac{2}{3}J_2}$$

J_2 is distortional energy

Zoback MD, 2007, Reservoir Geomechanics, Cambridge University Press

Mogi-Coulomb failure criterion (Al-Ajmi & Zimmerman, 2005*)

SEOUL NATIONAL UNIVERSITY

- Another form
  - Linear form

$$|\tau_{oct}| = \frac{1}{3}\left\{(\sigma_1-\sigma_2)^2+(\sigma_2-\sigma_3)^2+(\sigma_3-\sigma_1)^2\right\}^{1/2} = \frac{\sqrt{2}}{3}\left\{I_1^2+3I_2\right\}^{1/2} = \sqrt{\frac{2}{3}J_2}$$

Octahedral shear stress

$$\tau_{oct} = f(\tau_{m2})$$

$$\tau_{oct} = a + b\tau_{m2}$$

$$\tau_{m2} = \frac{(\sigma_1+\sigma_3)}{2}$$

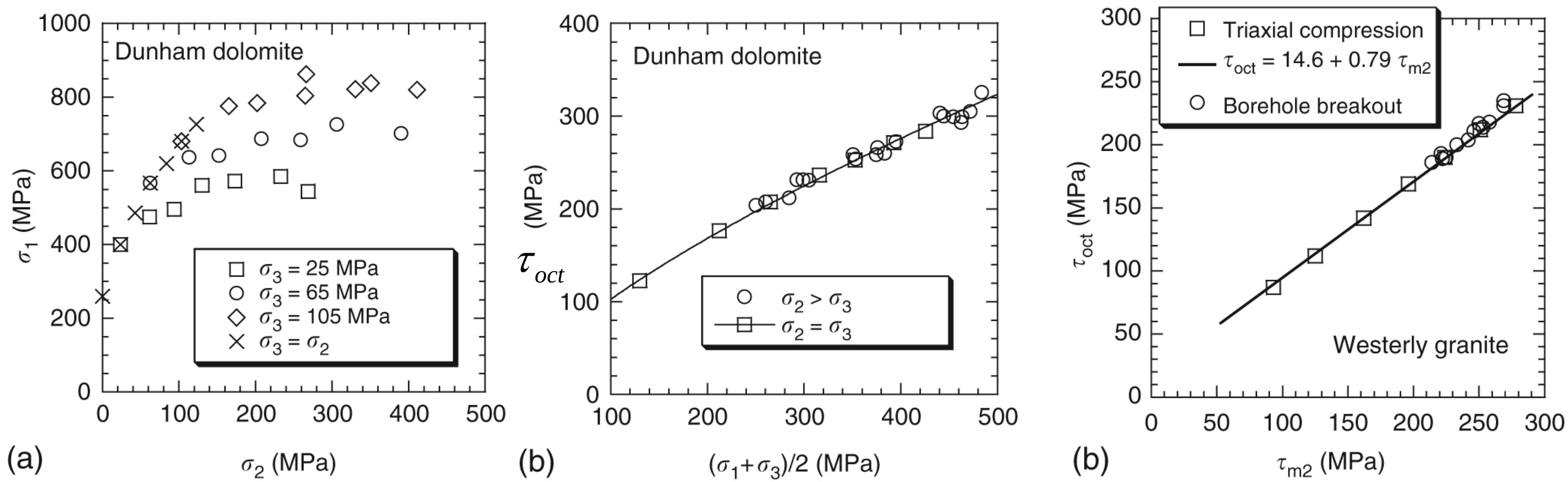

*Jaeger, Cook and Zimmerman, 2007, Fundamentals of Rock Mechanics, 4th ed., Blackwell Publishing

Strength and Pore Pressure

- Effective stress law has to be considered for evaluation of strength $\sigma' = \sigma - p_p$

$$S_1 = C_0 + nS_3 \quad (4.31)$$

where C_0, n and μ_i are 62.8 MPa, 2.82 and 0.54 for Berea sandstone and 40.8 MPa, 3.01 and 0.58 for Marianna limestone, respectively. Rearrangement of equation (4.31) yields the following

$$S_1 - S_3 = C_0 + (1 - n)P_p - (1 - n)S_3 \quad (4.32)$$

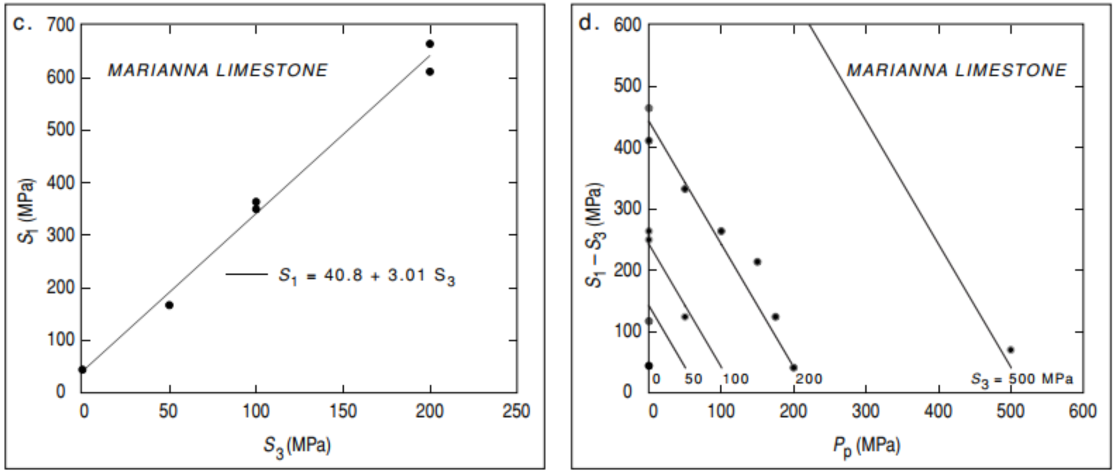

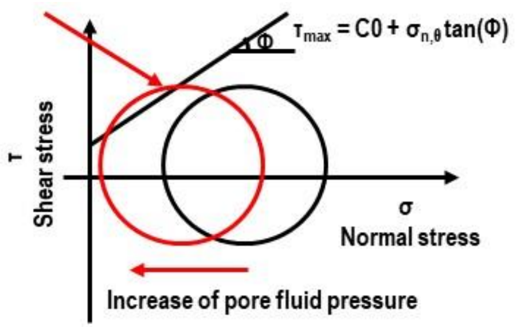

Figure 4.11. (a) Dependence of rock strength on confining pressure in the absence of pore pressure for Berea sandstone. (b) Dependence of strength on confining pressure and pore pressure assuming the simple Terzaghi effective stress law (equation 3.8) is valid (straight diagonal lines). (c) and (d) show similar data for Marianna limestone. Data derived from Handin, Hager *et al*. (1963).

Zoback MD, 2007, Reservoir Geomechanics, Cambridge University Press

Brittle vs. Ductile
The stress-strain curve – Brittle vs. Ductile

- Brittle vs ductile
  - Ductile: rock support an increasing load as it deforms
  - Brittle: load decreases as the strain increases
- Brittle-ductile transition
  - Rock becomes more ductile with increasing confining pressure

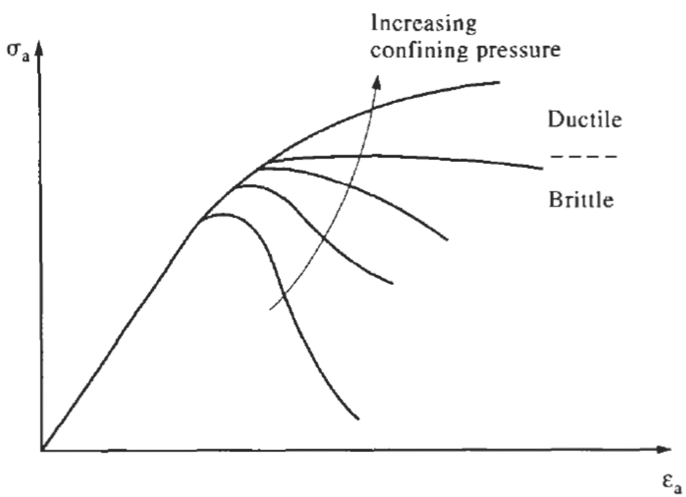

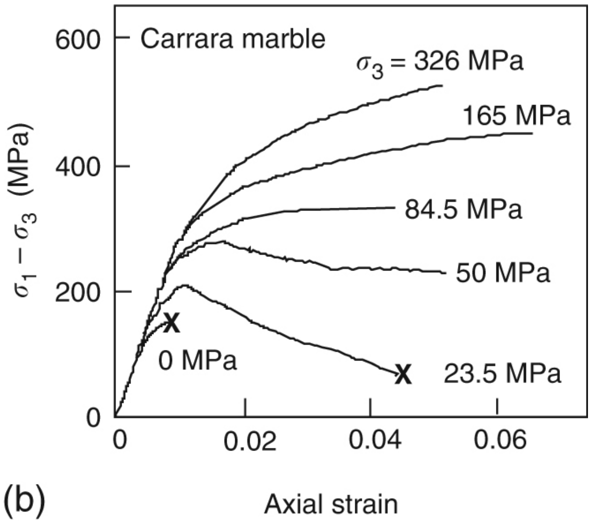

(b)

Hudson & Harrison, 1997, Engineering Rock Mechanics – An introduction to the principles, Pergamon

Jaeger, Cook and Zimmerman, 2007, Fundamentals of Rock Mechanics, 4th ed., Blackwell Publishing

Rock Strength Anisotropy

SEOUL NATIONAL UNIVERSITY

- Strength anisotropy
  - Weak bedding planes can affect strength

The maximum stress at which failure will occur, σ_1, will depend on σ_3, S_w, and σ_w by

$$\sigma_1 = \sigma_3 \frac{2(S_w + \mu_w \sigma_3)}{(1 - \mu_w \cot \beta_w) \sin 2\beta} \quad (4.33)$$

This is shown in Figure 4.12c. At high and low β, the intact rock strength (shown normalized by S_w) is unaffected by the presence of the bedding planes. At $\beta \sim 60°$, the strength is markedly lower. Using

$$\tan 2\beta_w = \frac{1}{\mu_w}$$

it can be shown that the minimum strength is given by

$$\sigma_1^{min} = \sigma_3 + 2(S_w + \mu_w \sigma_3)\left[(\mu_w^2)^{\frac{1}{2}} + \mu_w\right] \quad (4.34)$$

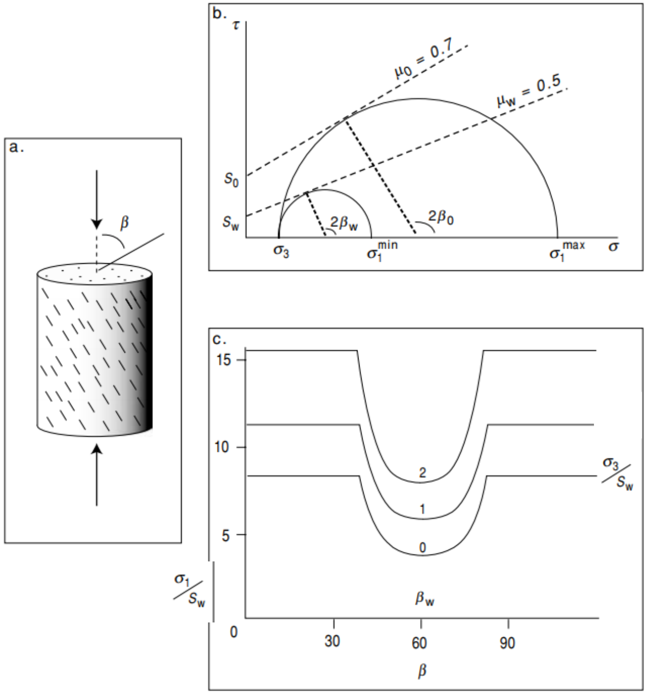

Figure 4.12. Dependence of rock strength on the angle of weak bedding or foliation planes. (a) Rock samples can be tested with the orientation of weak planes at different angles, β, to the maximum principal stress, σ_1. (b) The strength can be defined in terms of the intact rock strength (when the weak planes do not affect failure) and the strength of the weak planes. (c) Prediction of rock strength (normalized by the cohesion of bedding planes) as function of β. Modified from Donath (1966) and Jaeger and Cook (1979).

Zoback MD, 2007, Reservoir Geomechanics, Cambridge University Press

Rock Strength Anisotropy

SEOUL NATIONAL UNIVERSITY

- Examples

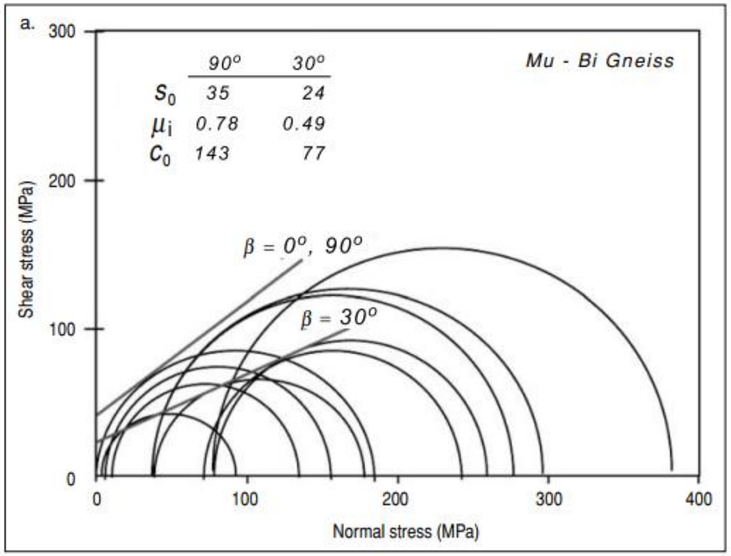

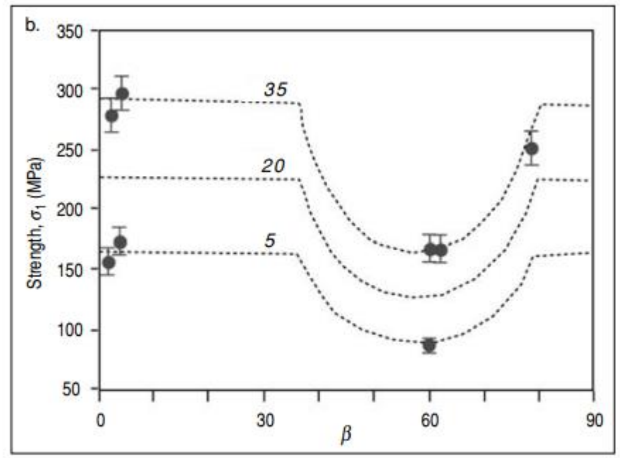

Figure 4.13. Fit of compressive strength tests to the theory illustrated in Figure 4.12 and defined by equation (4.33). Modified from Vernik, Lockner *et al.* (1992).

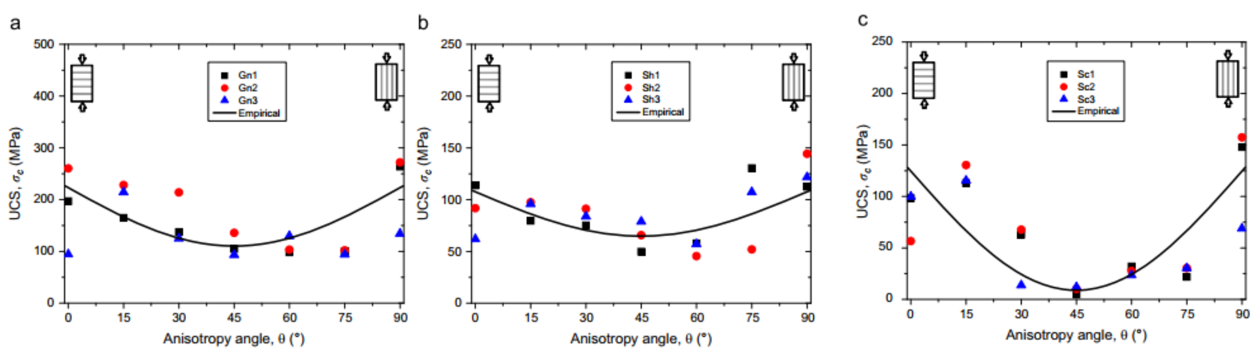

Cho JW, Kim H, Jeon S, Min KB, Deformation and strength anisotropy of Asan gneiss Boryeong shale, and Yeoncheon schist, IJRMMS, 2012;50:158-169.

Estimating rock strength from geophysical log data

SEOUL NATIONAL UNIVERSITY

- Why not directly measure?

Rock cutting from Pohang EGS site (4.3 km). ~few mm

REALITY

DREAM

One of the biggest rock core in the world at AECL URL in Canada (2002). ~ 1m

Obtaining rock core is a difficult and expensive job

Estimating rock strength from geophysical log data (Chang et al., 2006)

SEOUL NATIONAL UNIVERSITY

- V_p (or $\Delta t = V_p^{-1}$)
- Young's modulus (from Vp and density data)
- Porosity (from density log)

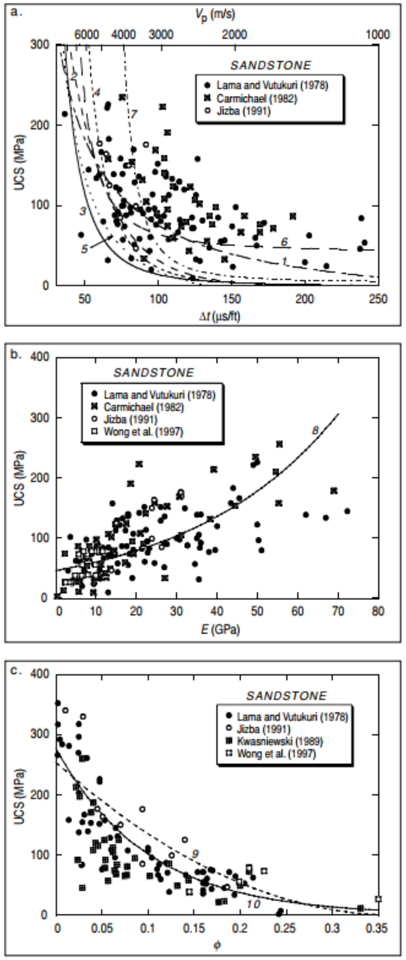

sandstone

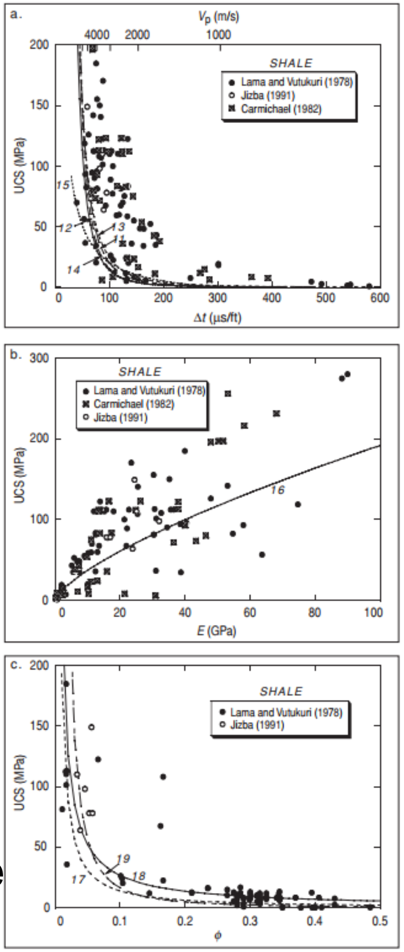

Shale

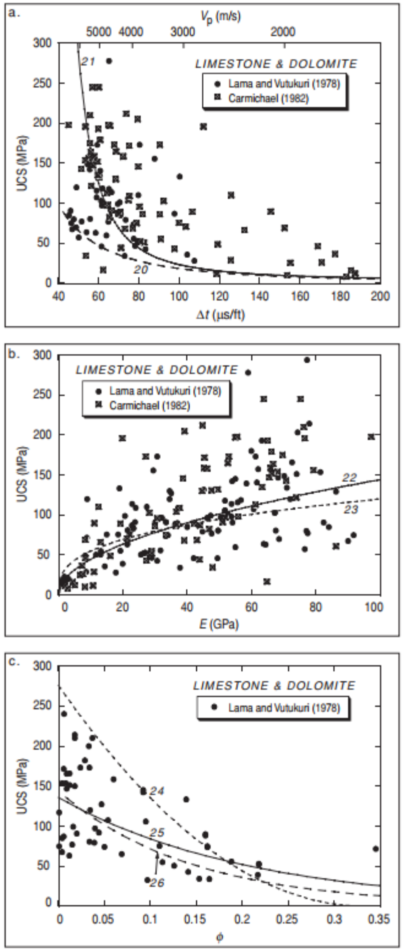

Limestone & dolomite

Zoback MD, 2007, Reservoir Geomechanics, Cambridge University Press

Estimating rock strength from geophysical log data

SEOUL NATIONAL UNIVERSITY

Table 4.1. *Empirical relationships between UCS and other physical properties in sandstones. After Chang, Zoback* et al. *(2006)*. Reprinted with permission of Elsevier

Equation No.	UCS, MPa	Region where developed	General comments	Reference
1	$0.035\ V_p - 31.5$	Thuringia, Germany	–	(Freyburg 1972)
2	$1200\ \exp(-0.036\Delta t)$	Bowen Basin, Australia	Fine grained, both consolidated and unconsolidated sandstones with wide porosity range	(McNally 1987)
3	$1.4138 \times 10^7\ \Delta t^{-3}$	Gulf Coast	Weak and unconsolidated sandstones	Unpublished
4	$3.3 \times 10^{-20}\ \rho^2 V_p^2\ [(1+\nu)/(1-\nu)]^2(1-2\nu)\ [1+0.78V_{clay}]$	Gulf Coast	Applicable to sandstones with UCS >30 MPa	(Fjaer, Holt *et al.* 1992)
5	$1.745\times10^{-9}\ \rho V_p^2 - 21$	Cook Inlet, Alaska	Coarse grained sands and conglomerates	(Moos, Zoback *et al.* 1999)
6	$42.1\ \exp(1.9 \times 10^{-11}\ \rho V_p^2)$	Australia	Consolidated sandstones with $0.05 < \phi < 0.12$ and UCS > 80MPa	Unpublished
7	$3.87\ \exp(1.14 \times 10^{-10}\ \rho V_p^2)$	Gulf of Mexico	–	Unpublished
8	$46.2\ \exp(0.000027E)$	–	–	Unpublished
9	$A\ (1-B\phi)^2$	Sedimentary basins worldwide	Very clean, well consolidated sandstones with $\phi < 0.30$	(Vernik, Bruno *et al.* 1993)
10	$277\ \exp(-10\phi)$	–	Sandstones with $2 <$ UCS < 360 MPa and $0.002 < \phi < 0.33$	Unpublished

Units used: V_p (m/s), Δt (μs/ft), ρ (kg/m^3), V_{clay} (fraction), E (MPa), ϕ (fraction)

Zoback MD, 2007, Reservoir Geomechanics, Cambridge University Press

Estimating rock strength from geophysical log data

SEOUL NATIONAL UNIVERSITY

Table 4.2. *Empirical relationships between UCS and other physical properties in shale. After Chang, Zoback* et al. *(2006)*. Reprinted with permission of Elsevier

	UCS, MPa	Region where developed	General comments	Reference
11	$0.77\,(304.8/\Delta t)^{2.93}$	North Sea	Mostly high porosity Tertiary shales	(Horsrud 2001)
12	$0.43\,(304.8/\Delta t)^{3.2}$	Gulf of Mexico	Pliocene and younger	Unpublished
13	$1.35\,(304.8/\Delta t)^{2.6}$	Globally	–	Unpublished
14	$0.5\,(304.8/\Delta t)^{3}$	Gulf of Mexico	–	Unpublished
15	$10\,(304.8/\Delta t - 1)$	North Sea	Mostly high porosity Tertiary shales	(Lal 1999)
16	$0.0528E^{0.712}$	–	Strong and compacted shales	Unpublished
17	$1.001\phi^{-1.143}$	–	Low porosity ($\phi < 0.1$), high strength shales	(Lashkaripour and Dusseault 1993)
18	$2.922\phi^{-0.96}$	North Sea	Mostly high porosity Tertiary shales	(Horsrud 2001)
19	$0.286\phi^{-1.762}$	–	High porosity ($\phi > 0.27$) shales	Unpublished

Units used: Δt (μs/ft), E (MPa), ϕ (fraction)

Zoback MD, 2007, Reservoir Geomechanics, Cambridge University Press

Estimating rock strength from geophysical log data

SEOUL NATIONAL UNIVERSITY

Table 4.3. *Empirical relationships between UCS and other physical properties in limestone and dolomite. After Chang, Zoback* et al. *(2006).* Reprinted with permission of Elsevier

	UCS, MPa	Region where developed	General comments	Reference
20	$(7682/\Delta t)^{1.82} / 145$	–	–	(Militzer 1973)
21	$10^{(2.44 + 109.14/\Delta t)} / 145$	–	–	(Golubev and Rabinovich 1976)
22	$0.4067\ E^{0.51}$	–	Limestone with 10 < UCS < 300 MPa	Unpublished
23	$2.4\ E^{0.34}$	–	Dolomite with 60 < UCS < 100 MPa	Unpublished
24	$C\ (1-D\phi)^2$	Korobcheyev deposit, Russia	C is reference strength for zero porosity (250 < C < 300 MPa). D ranges between 2 and 5 depending on pore shape	(Rzhevsky and Novick 1971)
25	$143.8\ \exp(-6.95\phi)$	Middle East	Low to moderate porosity (0.05 < ϕ < 0.2) and high UCS (30 < UCS < 150 MPa)	Unpublished
26	$135.9\ \exp(-4.8\phi)$	–	Representing low to moderate porosity (0 < ϕ < 0.2) and high UCS (10 < UCS < 300 MPa)	Unpublished

Units used: Δt (μs/ft), E (MPa), ϕ (fraction)

Zoback MD, 2007, Reservoir Geomechanics, Cambridge University Press

Estimating rock strength from geophysical log data

SEOUL NATIONAL UNIVERSITY

- Angle of internal friction

Table 4.4. *Empirical relationships between Φ and other logged measurements. After Chang, Zoback* et al. *(2006)*. Reprinted with permission of Elsevier

	Φ degree	General comments	Reference
27	$\sin^{-1}((V_p-1000)\ /\ (V_p+1000))$	Applicable to shale	(Lal 1999)
28	$70 - 0.417GR$	Applicable to shaly sedimentary rocks with $60 < GR < 120$	Unpublished

Units used: V_p (m/s), GR (API)

Zoback MD, 2007, Reservoir Geomechanics, Cambridge University Press

Estimating rock strength from geophysical log data

- Example at Gulf of Mexico

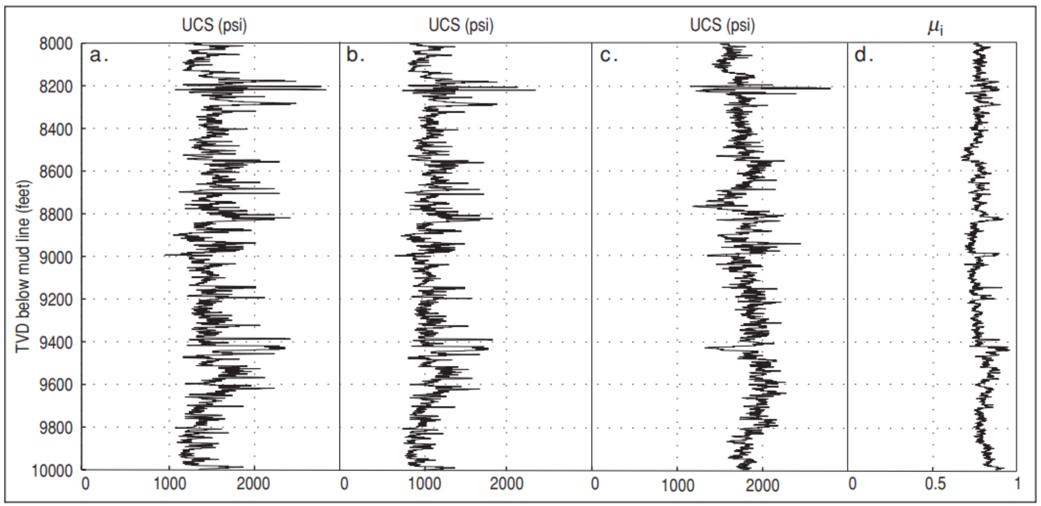

Figure 4.17. Utilization of equations (11) (a), (12) (b) and (19) (c) from Table 4.2, to predict rock strength for a shale section of a well drilled in the Gulf of Mexico. (d) The coefficient of internal friction is from equation (28) in Table 4.4. After Chang, Zoback *et al.* (2006). *Reprinted with permission of Elsevier.*

	UCS, MPa	Region where developed	General comments	Reference
11	$0.77\,(304.8/\Delta t)^{2.93}$	North Sea	Mostly high porosity Tertiary shales	(Horsrud 2001)
12	$0.43\,(304.8/\Delta t)^{3.2}$	Gulf of Mexico	Pliocene and younger	Unpublished
19	$0.286\phi^{-1.762}$	–	High porosity ($\phi > 0.27$) shales	Unpublished

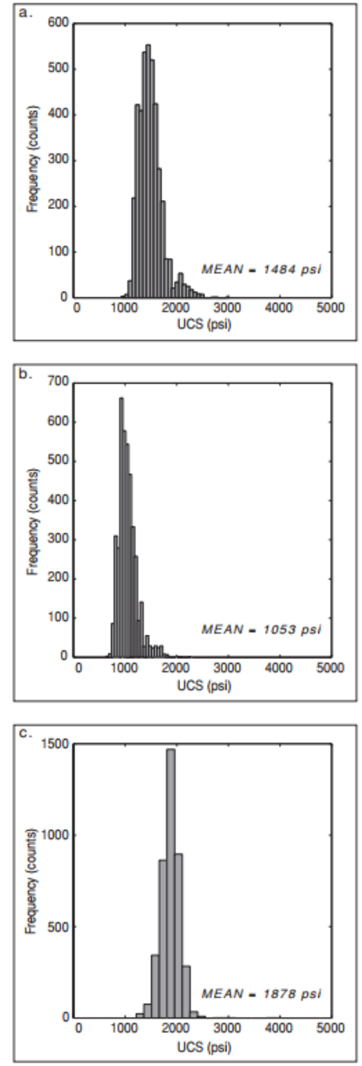

Figure 4.18. Histogram of shale strengths for the log-derived values shown in Figure 4.17: (a), (b) and (c) correspond to equations (11), (12) and (18) in Table 4.2, respectively. Note that the mean strength varies considerably, depending on which empirical relation is chosen. After Chang, Zoback *et al.* (2006). *Reprinted with permission of Elsevier.*

Zoback MD, 2007, Reservoir Geomechanics, Cambridge University Press

Shear enhanced compaction

SEOUL NATIONAL UNIVERSITY

- Shear-enhanced compaction
  - Irreversible deformation by the loss of porosity due to increased confining pressure and/or shear stress
  - Cam-Clay (Cambridge-Clay) model

$$p = \frac{1}{3}J_1 = \frac{1}{3}(\sigma_1 + \sigma_2 + \sigma_3)$$
$$p = \frac{1}{3}(S_1 + S_2 + S_3) - P_P \tag{4.35}$$

$$\underline{q} = \sqrt{3J_{2D}}$$
$$\underline{q}^2 = \frac{1}{2}[(S_1 - S_2)^2 + (S_2 - S_3)^2 + (S_1 - S_3)^2] \tag{4.36}$$

$$M^2p^2 - M^2p_0p + \underline{q}^2 = 0 \tag{4.37}$$

where M is known as the critical state line and can be expressed as $M = \underline{q}/p$.

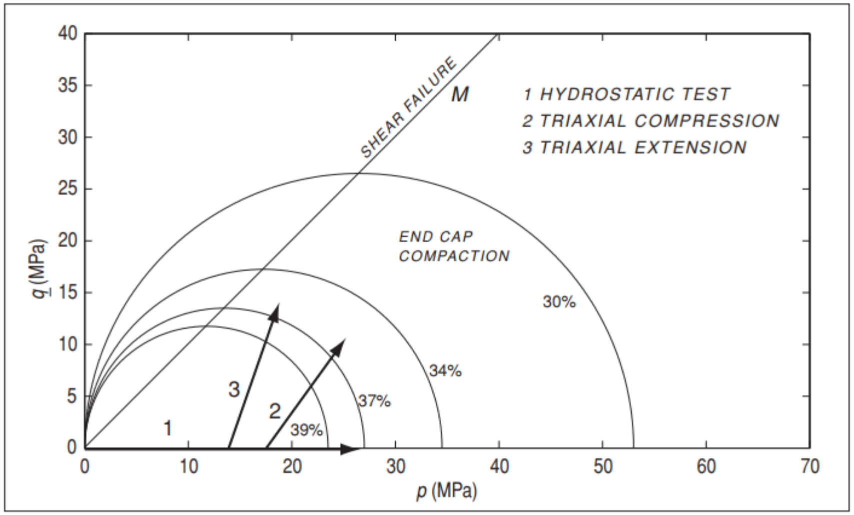

Figure 4.19. The Cam–Clay model of rock deformation is presented in p–$\underline{q}$ space as modified by Chan and Zoback (2002) following Desai and Siriwardane (1984) which allows one to define how inelastic porosity loss accompanies deformation. The contours defined by different porosities are sometimes called *end-caps*. Loading paths consistent with hydrostatic compression, triaxial compression and triaxial extension tests are shown. © *2002 Society Petroleum Engineers*

Zoback MD, 2007, Reservoir Geomechanics, Cambridge University Press

Shear enhanced compaction

- Example at sandstone

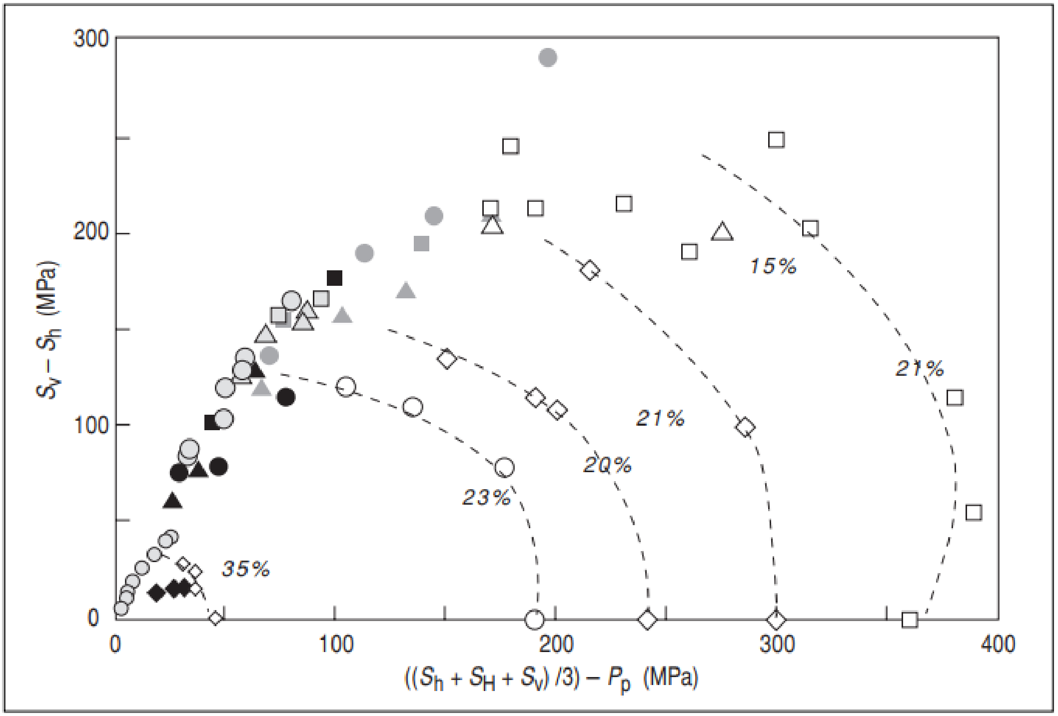

Figure 4.20. Compilation rock strength data for a wide variety of sandstones (different symbols) define the overall trend of irreversible porosity loss and confirms the general curvature of the end-caps to be similar to that predicted by the Cam-Clay model. After Schutjens, Hanssen *et al.* (2001). © *2001 Society Petroleum Engineers*

Zoback MD, 2007, Reservoir Geomechanics, Cambridge University Press

Tensile Strength

- Tensile strength (인장강도) : Maximum sustainable tensile stress

$$\sigma_t = \frac{T_{\max}}{A}$$

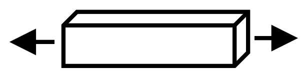

Tensile loading

- Measured by ‘Brazilian Test’ in case of rock (indirect tension, 간접인장)

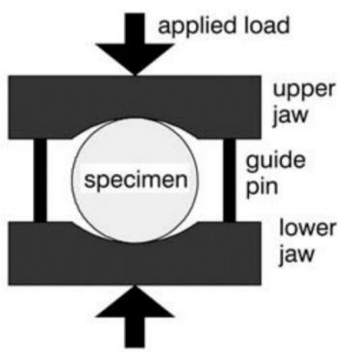

- <u>Tensile strength is 1/10 ~ 1/20 of UCS</u>

Tensile Rock Failure
Tensile Strength

- The reason why Brazilian Test Works…

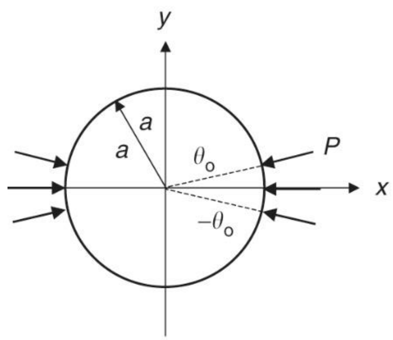

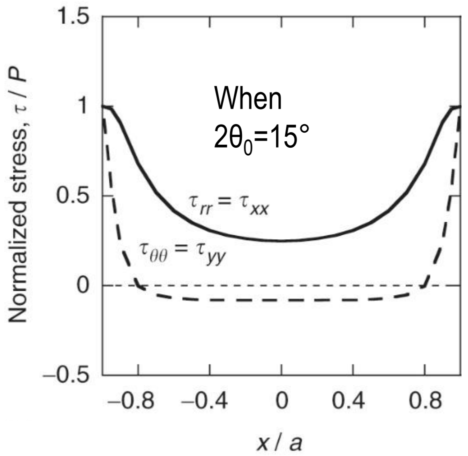

  - Stress distribution along the x-axis

$$\rho = r / a$$

$$\tau_{rr} = \frac{2P}{\pi}\left\{\frac{(1-\rho^2)\sin 2\theta_0}{(1-2\rho^2\cos 2\theta_0+\rho^4)} + \arctan\left[\frac{(1+\rho^2)}{(1-\rho^2)}\tan\theta_0\right]\right\} \qquad \tau_{\theta\theta} = -\frac{2P}{\pi}\left\{\frac{(1-\rho^2)\sin 2\theta_0}{(1-2\rho^2\cos 2\theta_0+\rho^4)} - \arctan\left[\frac{(1+\rho^2)}{(1-\rho^2)}\tan\theta_0\right]\right\}$$

Jaeger, Cook & Zimmerman, 2007, Fundamentals of Rock Mechanics, 4th ed, Blackwell Publishing

Tensile Rock Failure

SEOUL NATIONAL UNIVERSITY

- Stress intensity at the tip

$$K_\mathrm{i} = (P_\mathrm{f} - S_3)\pi L^{1/2} \tag{4.38}$$

where K_i is the stress intensity factor, P_f is the pressure within the fracture (taken to be uniform for simplicity), L is the length of the fracture and S_3 is the least principal stress. Fracture propagation will occur when the stress intensity factor K_i exceeds K_ic,

  - Fracture propagation $K_i > K_{ic}$
    - K_{ic}: fracture toughness (=critical stress intensity), MPa m$^{1/2}$
    - Important for propagation
  - Once fracture reaches a few tens of cm, small pressure in excess of S3 is required regardless of toughness.

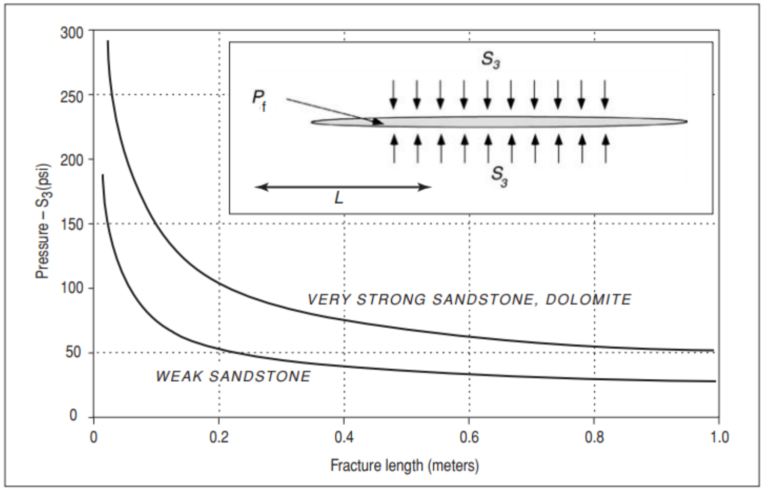

Figure 4.21. The difference between internal fracture pressure and the least principal stress as a function of fracture length for a Mode I fracture (see inset) for rocks with extremely high fracture toughness (such as very strong sandstone or dolomite) and very low fracture toughness (weakly cemented sandstone).

Zoback MD, 2007, Reservoir Geomechanics, Cambridge University Press

Tensile Rock Failure
Fracture toughness

SEOUL NATIONAL UNIVERSITY

- Crack-tip deformation mode
  - Mode I: crack opening model – mostly relevant to Hydraulic Fracturing
  - Mode II: sliding model
  - Mode III: tearing model

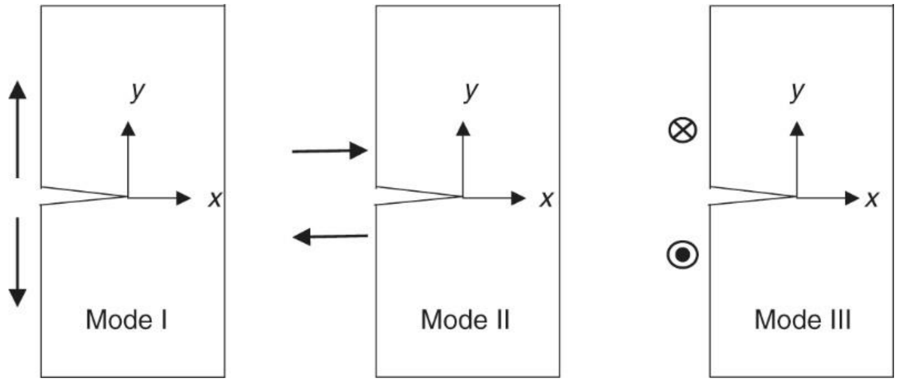

Jaeger, Cook & Zimmerman, 2007, Fundamentals of Rock Mechanics, 4th ed, Blackwell Publishing

Shear failure and the frictional strength of rocks

- Slip on fault (fracture)
  - Earthquake
  - Well casing failure
  - Induced seismicity
  - Fluid flow

$$\frac{\tau}{\sigma_{\mathrm{n}}} = \mu$$

***μ*: Coefficient of friction**

$\sigma_n = S_n - P_p$

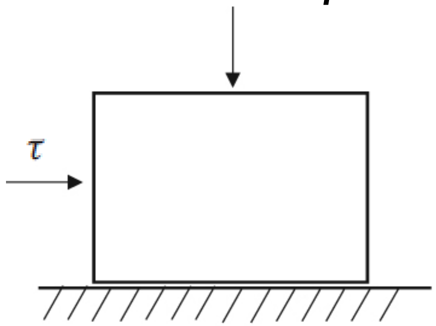

- Coulomb Failure Function

$$\mathrm{CFF} = \tau - \mu\sigma_{\mathrm{n}}$$

$$CFF = \tau - \mu(S_n - P_p)$$

When the Coulomb failure function is negative, a fault is stable as the shear stress is insufficient to overcome the resistance to sliding, $\mu\sigma_{\mathrm{n}}$. However, as CFF approaches zero, frictional sliding will occur on a pre-existing fault plane as there is sufficient shear stress to overcome the effective normal stress on the fault plane.

Shear failure and the frictional strength of rocks

SEOUL NATIONAL UNIVERSITY

- Shear failure of a fault (fracture)

$$\frac{\tau}{\sigma_n} = \mu$$

***μ*: Coefficient of friction**

$\sigma_n = S_n - P_p$

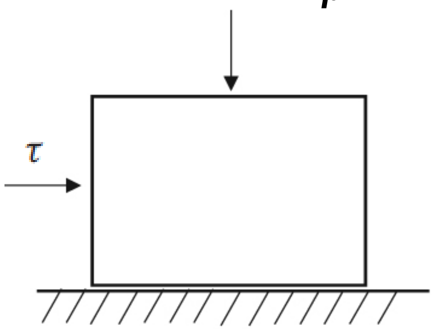

- Compressive (shear) failure of intact rock

$$\tau = S_0 + \sigma_n \mu_i$$

$$C_0 = 2S_0\left[\left(\mu_i^2+1\right)^{1/2} + \mu_i\right]$$

μ μ_i: **Coefficient of *internal* friction**

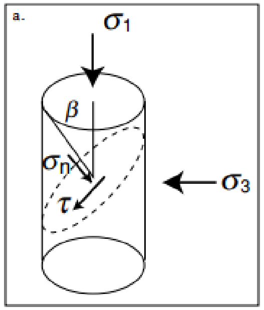

Zoback MD, 2007, Reservoir Geomechanics, Cambridge University Press

Shear failure and the frictional strength of rocks
Role of pore pressure

SEOUL NATIONAL UNIVERSITY

- Denver Earthquake (Healy et al., 1968)
  - ~ Magnitude 5.0 (1967)
  - Disposal of waste fluid from chemical-manufacturing operations
  - ~3,671 m depth
  - Earthquake within ~ 8 km of injection wells, no EQ before iniection

Table 1. Magnitude and frequency of occurrence of Denver earthquakes.

Year	Magnitude * 1.5–1.9	2.0–2.4	2.5–2.9	3.0–3.4	3.5–3.9	4.0–4.4	4.5–4.9	5.0–5.4	Total†
1962	72	29	4	2	1	1			189
1963	89	34	9	3	1	1			284
1964	26	8	6						72
1965	168	64	25	6	4				550
1966	61	18	3	2	1				186
1967	62	29	15	4	4	2		3	306
Total	478	182	62	17	11	4		3	1584
Average‡	83.2	30.5	9.4	2.6	1.4	0.4			

* To the nearest 0.1-magnitude unit. † Total includes all earthquakes reported. ‡ Average yearly activity 1962–66.

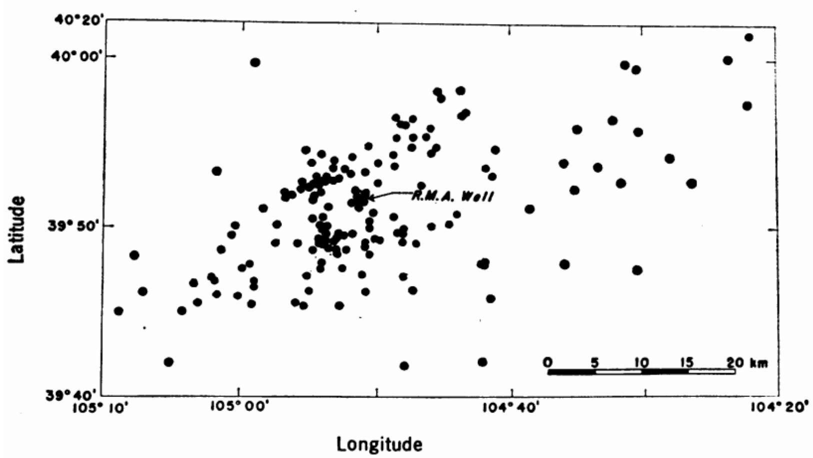

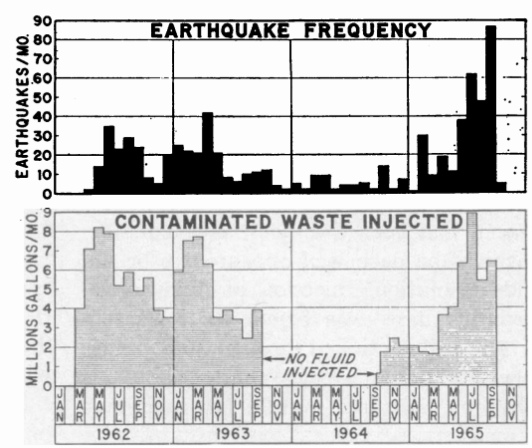

Injected volume: ~ 500,000 ton

Fig. 1. Observations on which David Evans in 1965 based his theory of the relation between fluid injection and earthquakes at the Rocky Mountain Arsenal, Denver, Colorado. (Left) Epicenters (solid circles) of earthquakes as calculated by Wang using data from the Bergen Park and Regis College stations and from temporary U.S. Geological Survey stations. (Right) Correlations, by Evans, between the number of earthquakes and the volume of fluid injected.

Healy, J. H., et al. (1968). "The Denver EarthquakeS." Science 161(3848): 1301-1310.

Shear failure and the frictional strength of rocks
Role of pore pressure

SEOUL NATIONAL UNIVERSITY

- Rocky Mountain Arsenal, Denver (Healy et al, 1968)
- Rangely Oil Field (Healy et al., 1976)
  - Weber sandstone, ~ 2,286 m
  - Fluid injection to improve productivity
  - Largest EQ magnitude: 3.1

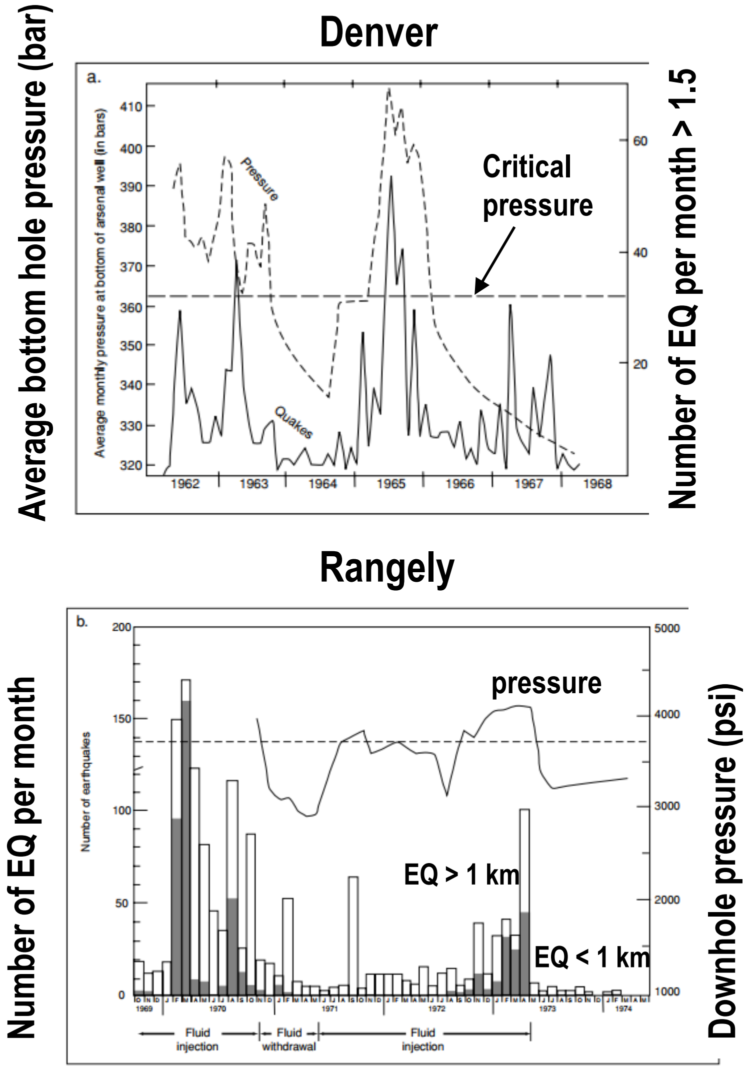

Figure 4.22. (a) Correlation between downhole pressure and earthquake occurrence during periods of fluid injection and seismicity at the Rocky Mountain Arsenal. Modified from Healy, Rubey *et al.* (1968). (b) Correlation between downhole pressure and earthquake occurrence triggered by fluid injection at the Rangely oil field in Colorado. After Raleigh, Healy *et al.* (1976).

Zoback MD, 2007, Reservoir Geomechanics, Cambridge University Press

Shear failure and the frictional strength of rocks
Coefficient of friction

- Range of μ (Byerlee's law)
  - At higher effective stress (10 MPa)

$$0.6 \leq \mu \leq 1.0$$

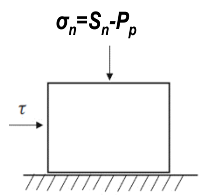

  - Coefficient of friction in genral lie in those ranges regardless of rock type and roughness
  - John Jaeger
    "There are only two things you need to know about friction. It is always 0.6 and it will always make a monkey out of you."
  - Shaly rock $\mu < 0.6$

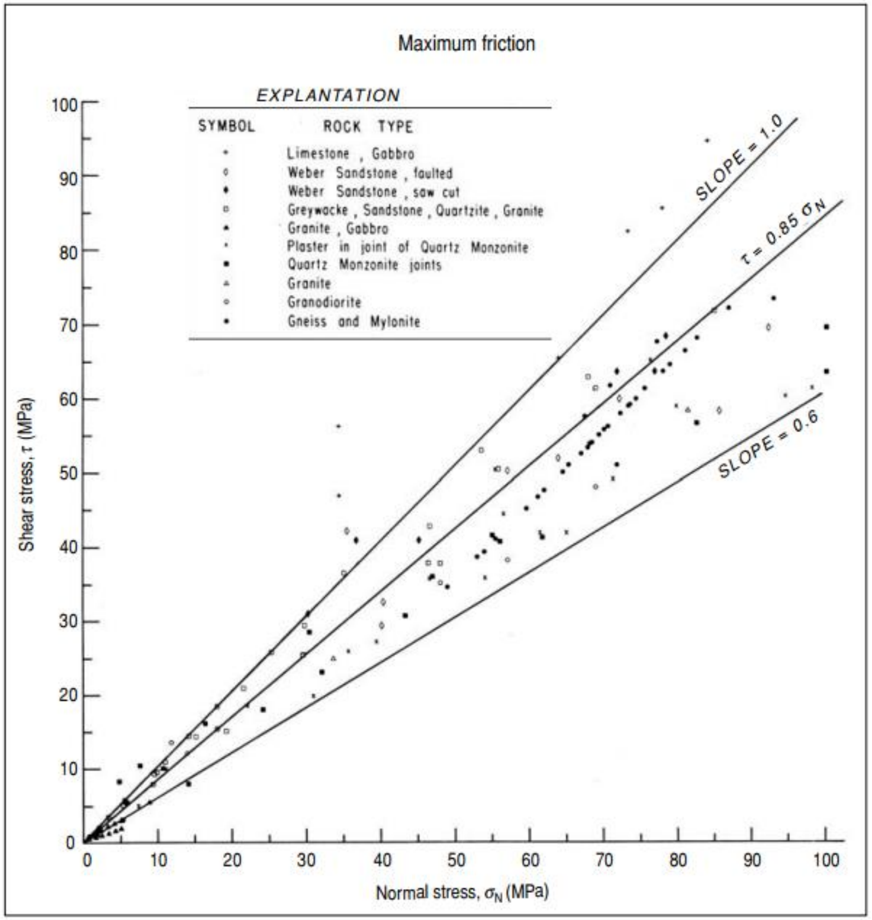

Figure 4.23. Rock mechanics tests on wide range of rocks (and plaster in a rock joint) demonstrating that the coefficient of friction (the ratio of shear to effective normal stress) ranges between 0.6 and 1.0 at effective confining pressures of interest here. Modified after Byerlee (1978).

Zoback MD, 2007, Reservoir Geomechanics, Cambridge University Press

The critically stressed crust

SEOUL NATIONAL UNIVERSITY

- Continental crust is generally in a state of incipient frictional failure
  - Widespread occurrence of EQ by reservoir impoundment
  - EQ triggered by small stress change
  - In situ stress measurement

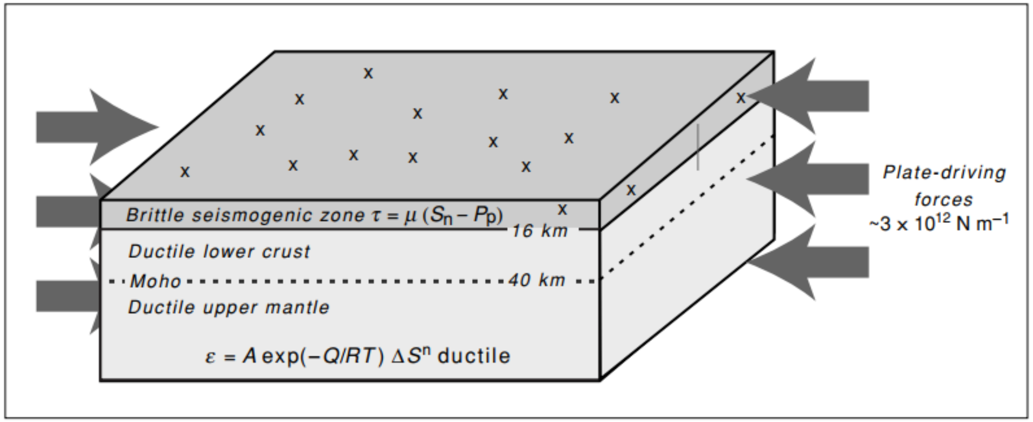

Figure 4.25. Schematic illustration of how the forces acting on the lithosphere keep the brittle crust in frictional equilibrium through creep in the lower crust and upper mantle (after Zoback and Townend 2001). *Reprinted with permission of Elsevier.*

Zoback MD, 2007, Reservoir Geomechanics, Cambridge University Press

The critically stressed crust

SEOUL NATIONAL UNIVERSITY

- Widespread occurrence of EQ by reservoir impoundmen
  - Small pore pressure change trigger EQ

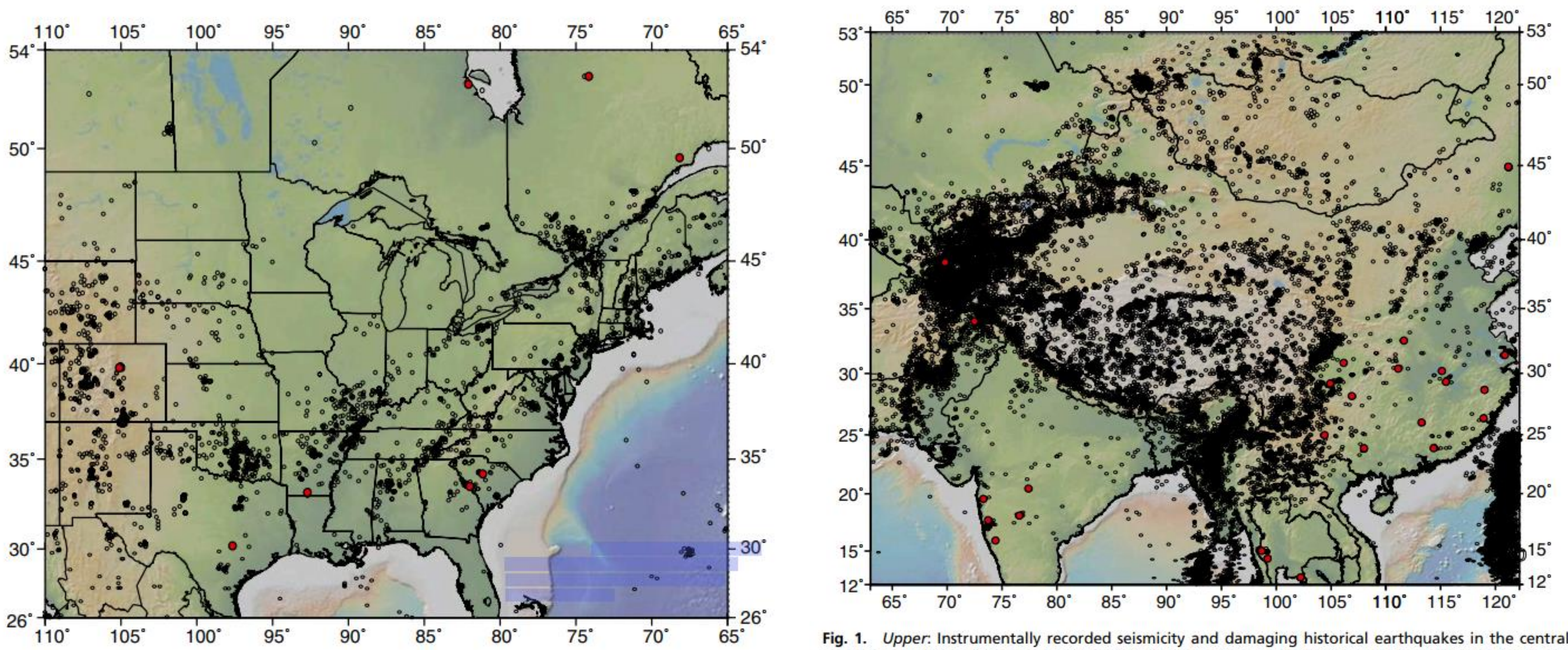

Fig. 1. *Upper*: Instrumentally recorded seismicity and damaging historical earthquakes in the central and eastern United States and southeastern Canada. Red dots indicate sites of reservoir-induced seismicity. *Lower*: Seismicity of south and east Asia and sites of reservoir-induced seismicity. Both data sets are available from the US Geological Survey (4).

Zoback, M. D. and S. M. Gorelick (2012). "Earthquake triggering and large-scale geologic storage of carbon dioxide." Proceedings of the National Academy of Sciences: 10164-10168.

The critically stressed crust

SEOUL NATIONAL UNIVERSITY

- EQ triggered by small stress change
  - Experiment at KTB borehole in Germany

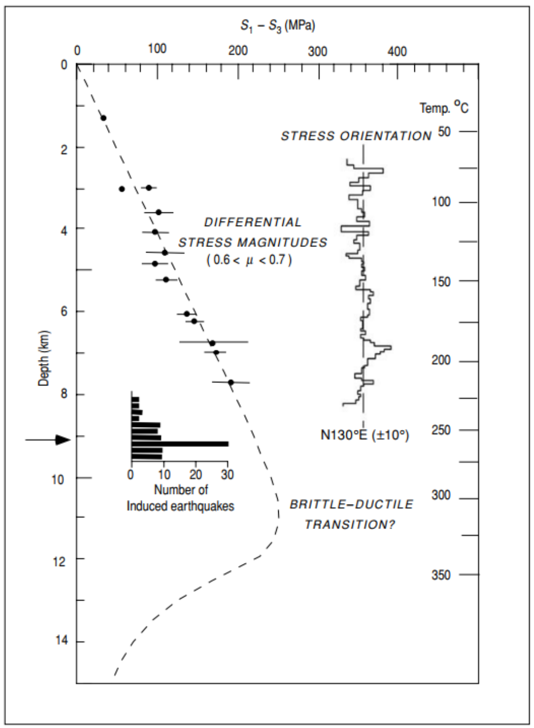

Figure 4.24. Stress measurements in the KTB scientific research well indicate a *strong* crust, in a state of failure equilibrium as predicted by Coulomb theory and laboratory-derived coefficients of friction of 0.6–0.7 (after Zoback and Harjes 1997). The arrow at 9.2 km depth indicates where the fluid injection experiment occurred.

- In situ stress measurement
  - Byerlee's law seems to work
  - Earth crust appears to be in a state of (failure) equilibrium

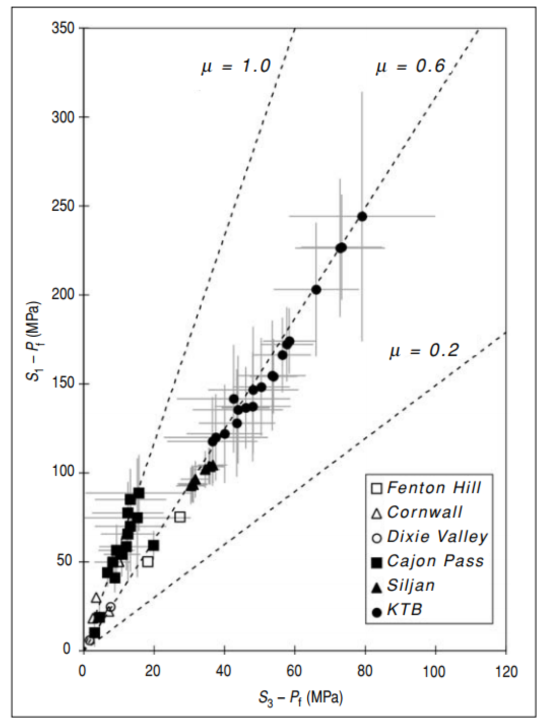

Figure 4.26. *In situ* stress measurements in relatively deep wells in crystalline rock indicate that stress magnitudes seem to be controlled by the frictional strength of faults with coefficients of friction between 0.6 and 1.0. After Zoback and Townend (2001). *Reprinted with permission of Elsevier.*

Zoback MD, 2007, Reservoir Geomechanics, Cambridge University Press

Limits on in situ stress from the frictional strength of faults

SEOUL NATIONAL UNIVERSITY

- Normal and shear stress at fractures

$$\tau_f = 0.5(\sigma_1 - \sigma_3)\sin 2\beta$$
$$\sigma_n = 0.5(\sigma_1 + \sigma_3) + 0.5(\sigma_1 - \sigma_3)\cos 2\beta$$

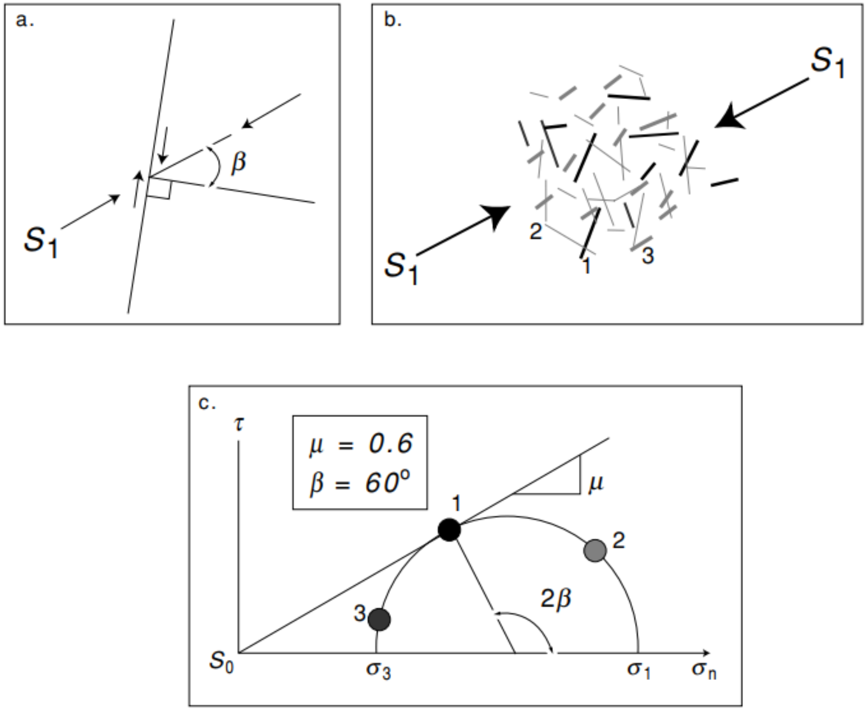

Figure 4.27. (a) Frictional sliding on an optimally oriented fault in two dimensions. (b) One can consider the Earth's crust as containing many faults at various orientations, only some of which are optimally oriented for frictional sliding. (c) Mohr diagram corresponding to faults of different orientations. The faults shown by black lines in (b) are optimally oriented for failure (labeled 1 in b and c), those shown in light gray in (b) (and labeled 2 in b and c) in (b) trend more perpendicular to S_{Hmax}, and have appreciable normal stress and little shear stress. The faults shown by heavy gray lines and labeled 3 in (b) are more parallel to S_{Hmax} have significantly less shear stress and less normal stress than optimally oriented faults as shown in (c).

- Optimally oriented fracture

β = 45°+1/2 tan$^{-1}\mu$

- μ = 1, β=67.5°
- μ = 0.6, β~60°
- μ ~ 0, β~45°

Zoback MD, 2007, Reservoir Geomechanics, Cambridge University Press

Limits on in situ stress from the frictional strength of faults

SEOUL NATIONAL UNIVERSITY

- Orientation of fault

$\beta = 45° + 1/2 \tan^{-1}\mu$

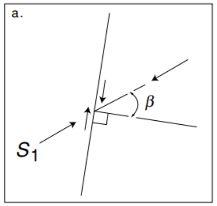

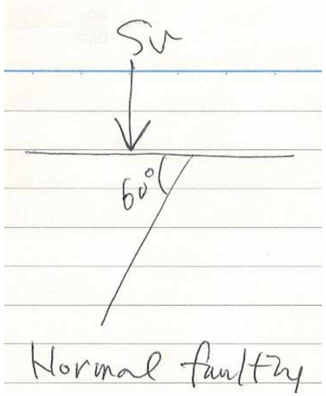

- Normal faults are expected to form in conjugate pairs that dip ~60° and strike parallel to the direction of S_{Hmax}.
- Strike-slip faults are expected to be vertical and form in conjugate pairs that strike ~30° from the direction of S_{Hmax}.
- Reverse faults are expected to dip ~30° and form in conjugate pairs that strike normal to the direction of S_{Hmax}.

Jaeger and Cook (1979) showed that the values of σ_1 and σ_3 (and hence S_1 and S_3) that corresponds to the situation where a critically oriented fault is at the frictional limit (*i.e.* equation 4.39 is satisfied) are given by:

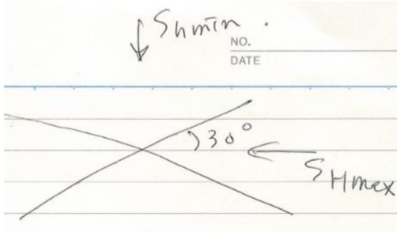

- Effective stress ratio
  - At optimal orientation

$$\frac{\sigma_1}{\sigma_3} = \frac{S_1 - P_p}{S_3 - P_p} = [(\mu^2 + 1)^{1/2} + \mu]^2$$

such that for $\mu = 0.6$ (see Figure 4.26),

$$\frac{\sigma_1}{\sigma_3} = 3.1$$

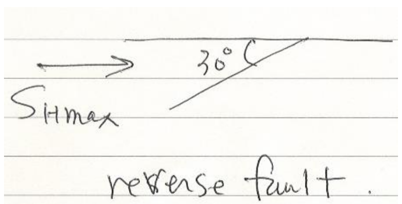

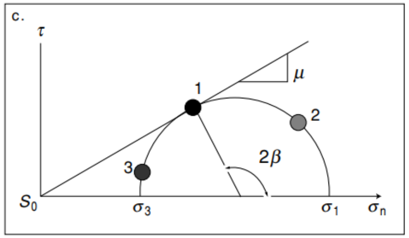

Zoback MD, 2007, Reservoir Geomechanics, Cambridge University Press

Limits on in situ stress from the frictional strength of faults

- Range of stress magnitude (hydrostatic pore pressure)

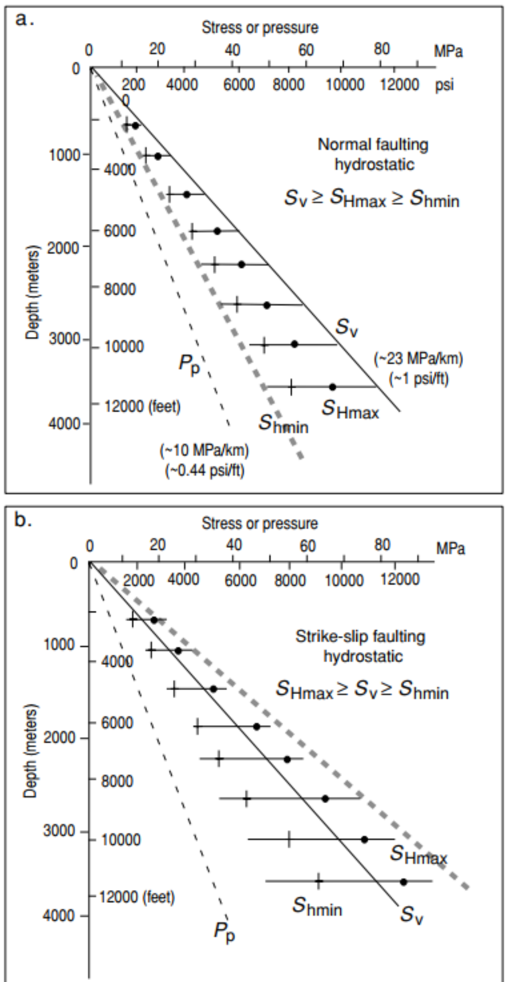

$$\text{Normal faulting } \frac{\sigma_1}{\sigma_3} = \frac{S_v - P_p}{S_{hmin} - P_p} \leq [(\mu^2+1)^{1/2}+\mu]^2$$

$$\text{Strik-slip faulting } \frac{\sigma_1}{\sigma_3} = \frac{S_{Hmax} - P_p}{S_{hmin} - P_p} \leq [(\mu^2+1)^{1/2}+\mu]^2$$

$$\text{Reverse faulting } \frac{\sigma_1}{\sigma_3} = \frac{S_{Hmax} - P_p}{S_v - P_p} \leq [(\mu^2+1)^{1/2}+\mu]^2$$

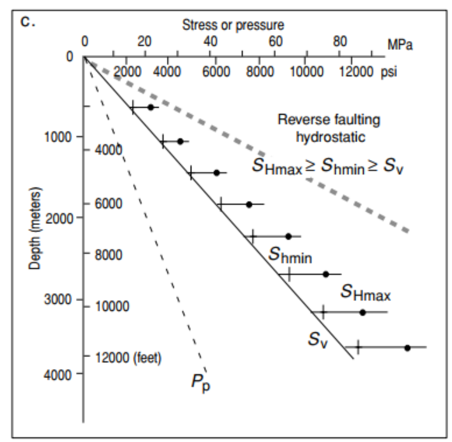

Figure 4.28. Limits on stress magnitudes defined by frictional faulting theory in normal (a), strike-slip and (b) reverse faulting (c) regimes assuming hydrostatic pore pressure. The heavy line in (a) shows the minimum value of the least principal stress, S_{hmin}, in normal faulting environments, in (b) the maximum value of S_{Hmax} for the values of S_{hmin} shown by the ticks and (c) the maximum value of S_{Hmax} for reverse faulting regimes where the least principal stress is the vertical stress S_v.

Zoback MD, 2007, Reservoir Geomechanics, Cambridge University Press

Limits on in situ stress from the frictional strength of faults

SEOUL NATIONAL UNIVERSITY

- Change of stress state due to the increase of pore pressure

Normal faulting $\frac{\sigma_1}{\sigma_3} = \frac{S_v - P_p}{S_{hmin} - P_p} \le [(\mu^2 + 1)^{1/2} + \mu]^2$

Strik-slip faulting $\frac{\sigma_1}{\sigma_3} = \frac{S_{Hmax} - P_p}{S_{hmin} - P_p} \le [(\mu^2 + 1)^{1/2} + \mu]^2$

Reverse faulting $\frac{\sigma_1}{\sigma_3} = \frac{S_{Hmax} - P_p}{S_v - P_p} \le [(\mu^2 + 1)^{1/2} + \mu]^2$

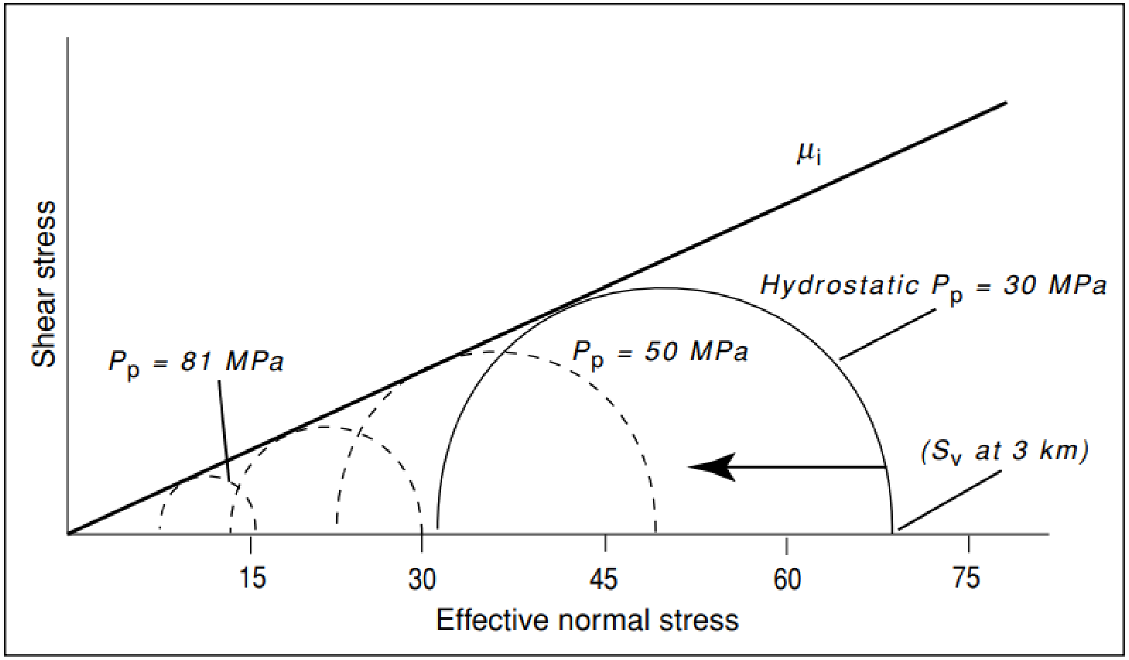

Figure 4.30. In terms of frictional faulting theory, as pore pressure increases (and effective stress decreases), the difference between the maximum and minimum effective principal stress (which defines the size of the Mohr circle) decreases with increasing pore pressure at the same depth.

Zoback MD, 2007, Reservoir Geomechanics, Cambridge University Press

Limits on in situ stress from the frictional strength of faults

SEOUL NATIONAL UNIVERSITY

- Range of stress magnitude (overpressure)

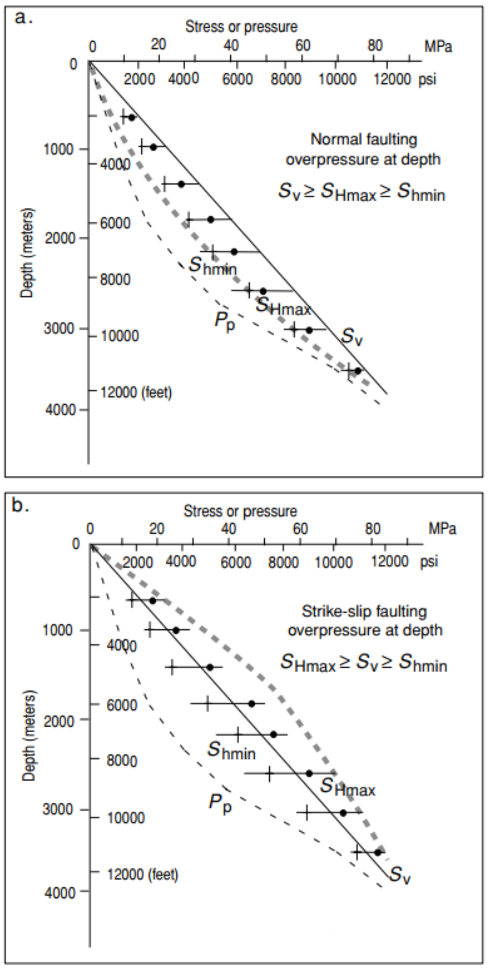

$$\text{Normal faulting } \frac{\sigma_1}{\sigma_3} = \frac{S_v - P_p}{S_{hmin} - P_p} \leq [(\mu^2+1)^{1/2}+\mu]^2$$

$$\text{Strik-slip faulting } \frac{\sigma_1}{\sigma_3} = \frac{S_{Hmax} - P_p}{S_{hmin} - P_p} \leq [(\mu^2+1)^{1/2}+\mu]^2$$

$$\text{Reverse faulting } \frac{\sigma_1}{\sigma_3} = \frac{S_{Hmax} - P_p}{S_v - P_p} \leq [(\mu^2+1)^{1/2}+\mu]^2$$

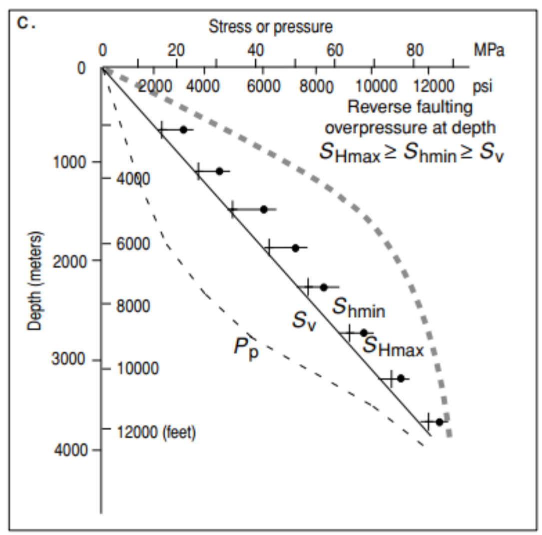

Figure 4.29. Same as Figure 4.28 when overpressure develops at depth as shown. Note that in all three stress states, when pore pressure is nearly lithostatic, all three principal stresses are also close to S_v.

Zoback MD, 2007, Reservoir Geomechanics, Cambridge University Press

Stress polygon

SEOUL NATIONAL UNIVERSITY

- Diagram showing the range of possible stress state at a given depth and pore pore pressure
  - Stress state above a $S_{Hmax} = S_{hmin}$

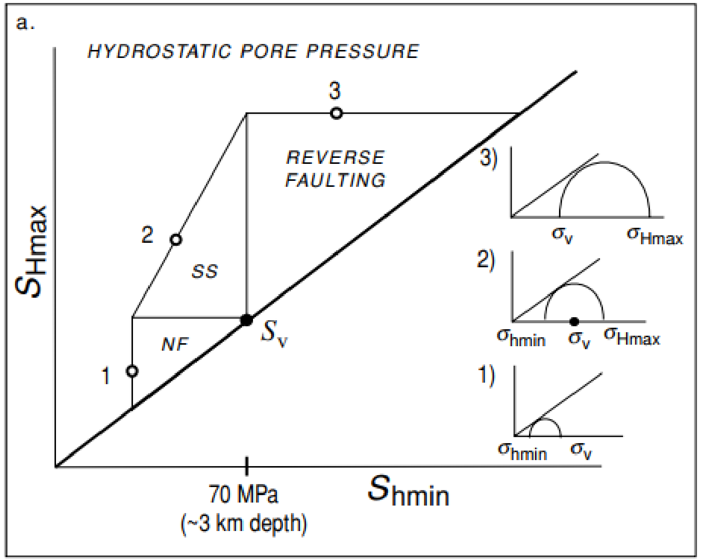

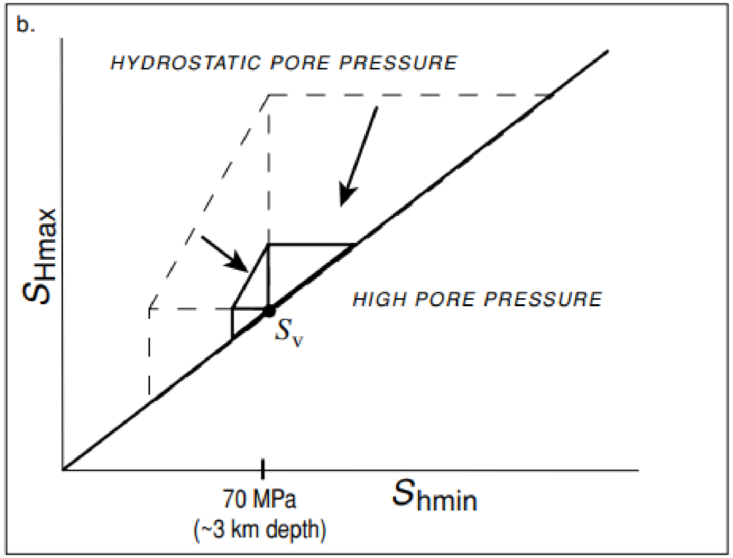

$$\text{Normal faulting } \frac{\sigma_1}{\sigma_3} = \frac{S_v - P_p}{S_{hmin} - P_p} \le [(\mu^2+1)^{1/2}+\mu]^2$$

$$\text{Strik-slip faulting } \frac{\sigma_1}{\sigma_3} = \frac{S_{Hmax} - P_p}{S_{hmin} - P_p} \le [(\mu^2+1)^{1/2}+\mu]^2$$

$$\text{Reverse faulting } \frac{\sigma_1}{\sigma_3} = \frac{S_{Hmax} - P_p}{S_v - P_p} \le [(\mu^2+1)^{1/2}+\mu]^2$$

Zoback MD, 2007, Reservoir Geomechanics, Cambridge University Press